Middle–Late Cretaceous climate of the southern high latitudes: Stable isotopic evidence for minimal equator-to-pole thermal gradients

Brian T. Huber *Department of Paleobiology, MRC-121, National Museum of Natural History, Smithsonian Institution, Washington, D.C. 20560*
David A. Hodell *Department of Geology, University of Florida, Gainesville, Florida 32611*
Christopher P. Hamilton* *Department of Paleobiology, MRC-121, National Museum of Natural History, Smithsonian Institution, Washington, D.C. 20560*

ABSTRACT

A detailed $\delta^{18}O$ and $\delta^{13}C$ stratigraphy has been generated from analysis of well-preserved Albian–early Maastrichtian foraminifera from Deep Sea Drilling Project (DSDP) Sites 511 and 327 (Falkland Plateau; ≈58°S–62°S paleolatitude) in the southern South Atlantic, and Cenomanian and Coniacian–Santonian foraminifera from DSDP Site 258 (Naturaliste Plateau; ≈58°S paleolatitude) in the southern Indian Ocean. These results, when combined with previously published Maastrichtian stable isotope data from Ocean Drilling Program (ODP) Site 690 (Weddell Sea, ≈65°S paleolatitude), provide new insight into the climatic and oceanographic history of the southern high latitudes during middle–Late Cretaceous time. The planktonic foraminifer $\delta^{18}O$ curves reveal a gradual warming of surface waters from the Albian through the Cenomanian followed by extremely warm surface waters from the Turonian through the early Campanian. Long-term cooling of surface waters began in the late early Campanian and continued through the end of the Maastrichtian. The benthic foraminifer $\delta^{18}O$ record generally parallels changes in the oxygen isotopic curves defined by shallow-dwelling planktonic foraminifera. The vertical oxygen and carbon isotopic gradients were relatively low during the Albian–Cenomanian, high from the Turonian–early Campanian, and then low during the late Campanian and Maastrichtian.

Foraminiferal oxygen isotopic data from published sources and this study are averaged for each site, corrected for latitudinal changes in salinity based on modern-day surface-water values, and plotted versus paleolatitude for the late Albian, Coniacian–Santonian, and late Maastrichtian. Differences between low- and high-latitude surface-water paleotemperatures are estimated at ≈14 °C during the late Albian and late Maastrichtian, but the Coniacian–Santonian reconstruction reveals only a 0–4 °C latitudinal temperature gradient. Uncertainty regarding Cretaceous salinity gradients and possible diagenetic alteration of $\delta^{18}O$ values introduce error into our estimates of paleolatitudinal thermal gradients; however, apparent low equator-to-pole temperature differences could indicate much higher poleward heat transport than at present.

INTRODUCTION

The climate of the Cretaceous Period has been characterized by numerous authors as substantially warmer than the present, generally ice free, and having markedly reduced vertical and latitudinal temperature gradients (Barron, 1983; Crowley and North, 1991; Frakes et al., 1992). In fact, the middle Cretaceous (Albian–Cenomanian) has been cited as the culmination of a warming trend that began 150 m.y. earlier in the Late Permian (Frakes, 1986). Evidence to support a middle Cretaceous thermal maximum is largely qualitative, based on a poleward habitat expansion of thermophilic marine organisms such as coral reefs, larger foraminifera, gastropods, and rudistid bivalves (Sohl, 1969; Kauffman, 1973; Gordon, 1973; Habicht, 1979; Lloyd, 1982); occurrence of dinosaurs of presumed warm weather affinity in the Arctic (Colbert, 1973) and Antarctica (Olivero et al., 1991); and poleward expansion of floral biogeographic provinces (Barnard, 1973; Vakhrameev, 1975). Terrestrial floral data, however, do not show a consistent climatic pattern. Paleotemperature estimates based on leaf physiognomy for the middle latitudes of North America (Fig. 1) indicate a gradual increase in mean annual temperature from the late Albian through Santonian, and a step-wise decrease into the early Maastrichtian followed by a temperature increase through the end of the Maastrichtian (Wolfe and Upchurch, 1987; Johnson and Hickey, 1990). In contrast, paleobotanical evidence from the Alaskan North Slope (Spicer and Parrish, 1986, 1987) suggests maximum warmth occurred during the Coniacian. Pollen studies from the same region indicate a significant cooling occurred during the late Maastrichtian (Frederiksen, 1989).

Although Cretaceous sediments have been recovered at >200 DSDP and ODP sites, oxygen isotope data are surprisingly limited. The only tropical sites that have been studied are DSDP Sites 47 and 305 in the western North Pacific (Douglas and Savin, 1973, 1975) and Sites 463 and 465 in the central North Pacific (Boersma and Shackleton, 1981). Despite the importance of these data, our knowledge of tropical paleotemperatures remains incomplete as geographic coverage is poor and stratigraphic coverage is discontinuous, especially for the Albian–Campanian.

Because the composite paleotemperature curve of Douglas and Savin (1973, 1975) spans the Berriasian–Maastrichtian, it has been widely cited in discussions of long-term climatic trends during the Cretaceous. These isotopic data suggest that surface and deep wa-

*Present address: Department of Geology, University of California at Davis, Davis, California 95616.

GSA Bulletin; October 1995; v. 107; no. 10; p. 1164–1191; 12 figures; 6 tables.

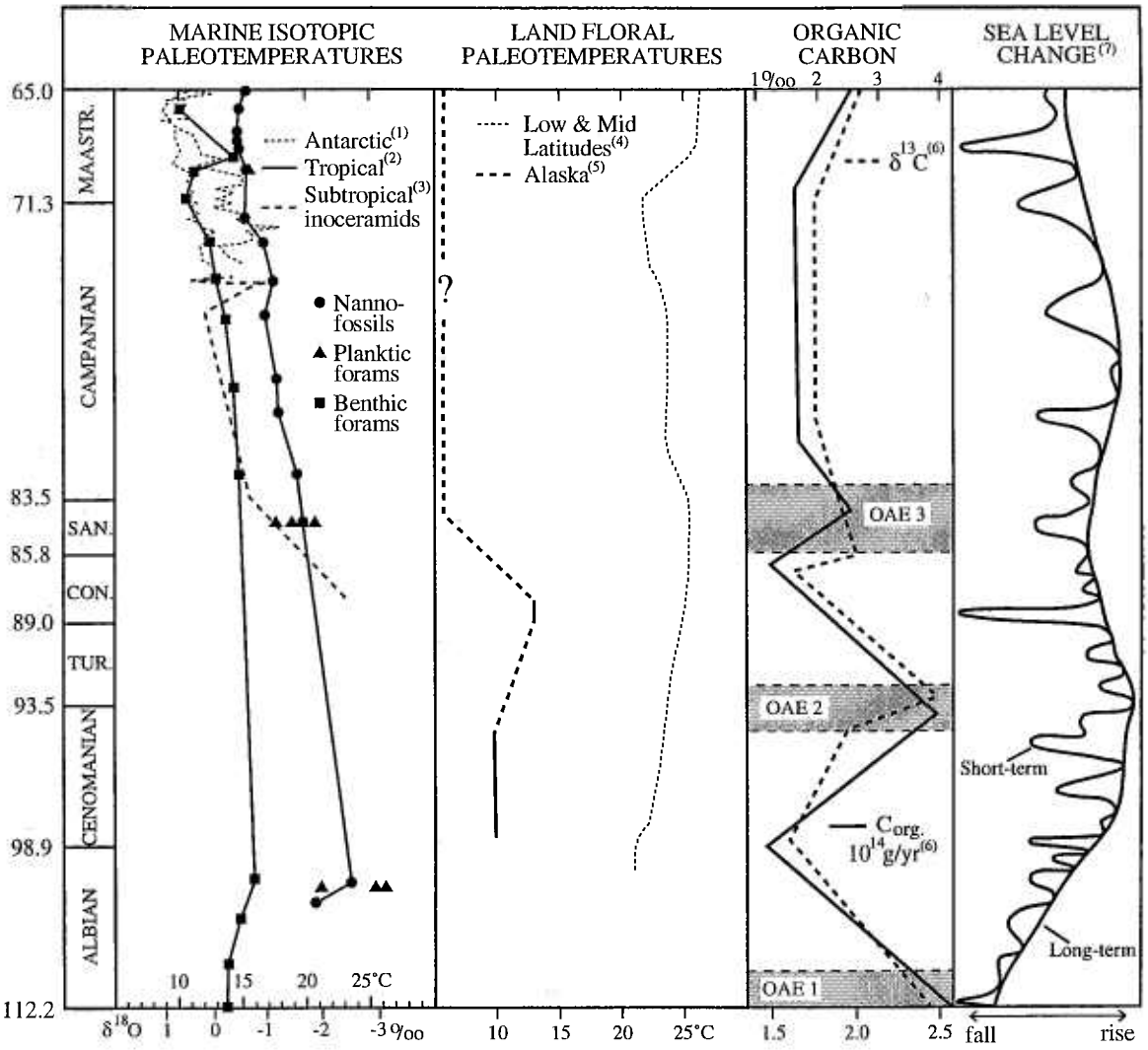

Figure 1. Previously published estimates of marine and terrestrial paleotemperature changes, trends in the burial rates and $\delta^{13}C$ composition of organic carbon, and estimates of relative sea-level change during Albian–Maastrichtian time. (1) Barrera and Huber (1990); (2) Douglas and Savin (1975); (3) Saltzman and Barron (1982); (4) Wolfe and Upchurch (1987); (5) Spicer and Parrish (1987); (6) Arthur et al. (1985); (7) modified from Haq et al. (1988). Shaded areas labeled OAE represent oceanic anoxic events identified by Scholle and Arthur (1980) and Arthur et al. (1985).

ters were warmest during the late Albian and coolest in the late Maastrichtian (Fig. 1). Most of the samples analyzed by Douglas and Savin (1973, 1975) were composed of fine-fraction bulk carbonate rather than monospecific foraminifera. Isotopic measurements of bulk carbonate are suspect because fine-fraction carbonate (nannofossils) is more susceptible to diagenetic alteration than is coarse-fraction carbonate (foraminifera), owing to the fact that nannofossils act as both donor and nucleation sites for secondary calcite precipitation (Schlanger and Douglas, 1974; Matter et al., 1975; Garrison, 1981; Nelson, 1986). Variation in the relative amounts of calcareous organisms analyzed in bulk carbonate samples also may affect the paleotemperature signal due to their differing vital effects.

Late Turonian–Maastrichtian paleotemperatures estimated from Sites 463 and 465 (Boersma and Shackleton, 1981) also depict a long-term cooling, with warmest surface and bottom waters during the Coniacian (≈24 and ≈18 °C, respectively) and coolest surface and bottom waters during the Maastrichtian (≈20 and ≈11 °C, respectively).

Isotopic paleotemperature estimates from subtropical (Saito and von Donk, 1974; Boersma, 1984; Oberhansli, 1986; D'Hondt and Lindinger, 1994) and Antarctic (Barrera et al., 1987; Barrera and Huber, 1990) marine sediments indicate cooling from the upper Campanian through the Maastrichtian, but provide few constraints regarding earlier times. Oxygen isotopic analyses of shell fragments of *Inoceramus* in the Angola Basin (DSDP hole 530A, subtropical South Atlantic) indicate remarkably warm deep water temperatures of ≈22 °C during the Coniacian and ≈15 °C during the late Santonian (Saltzman and Barron, 1982; Fig. 1). By late Campanian–

TABLE 1. CRITERIA USED FOR INDIRECT CORRELATION WITH EUROPEAN STAGE BOUNDARIES AND SUBDIVISIONS OF EUROPEAN STAGES AT SOUTHERN HIGH-LATITUDE SITES

Boundary level	Planktonic foraminifera	Calcareous nannoplankton	Magnetic anomaly	Age (Ma)
Maastrichtian–Paleocene	*Eoglobigerina* spp.*	*Biantholithus sparsus**	middle C29R	65.0
Upper–lower Maastrichtian	*Abathomphalus mayaroensis**	*Reinhardtites levis*†	middle C31R	69.4
Campanian–Maastrichtian	*Rugotruncana circumnodifer**	*Biscutum coronum*†	middle C32N	71.3
Upper–lower Campanian§	*Globigerinelloides impensus**	Uncertain	middle C33N	76.2
Santonian–Campanian§	Uncertain	*Eprolithus floralis*†	bottom C33R	83.5
Coniacian–Santonian§	Uncertain	*Micula decussata**	upper C34N	85.8
Turonian–Coniacian§	*Archaeoglobigerina cretacea**	*Marthasterites furcatus**	middle C34N	89.0
Cenomanian–Turonian§	*Whiteinella archaeocretacea**	*Eiffellithus eximius**	middle C34N	93.5
Albian–Cenomanian	*Schackoina* and *Praeglobotruncana**	Uncertain	middle C34N	98.9
Aptian–Albian	*Ticinella bejaouaensis*†	*Hayesites albiensis**	lower C34N	112.2

Note: Biostratigraphic datums used to approximate boundary levels are based on planktonic foraminifera (Bralower et al., 1994; Huber, 1992, unpublished data; R. M. Leckie, 1995, personal commun.) and calcareous nannofossils (Wise and Wind, 1983; Wind and Wise, 1983; Bralower, 1992; D. K. Watkins, 1995, personal commun.; J. J. Pospichal, 1995, personal commun.). Entries on same line do not indicate synchroneity of foraminifer and nannofossil datums. Geomagnetic polarity and stratigraphic time scale are from Gradstein et al. (1994).

*FAD (first appearance datum).

†LAD (last appearance datum).

§High-latitude boundary poorly determined.

early Maastrichtian time, Hole 530A data indicate that bottom waters had cooled to 8–10 °C. As these temperatures are considerably warmer than estimates determined for bottom waters in surrounding shallower ocean basins, Saltzman and Barron (1982) suggested that the Angola Basin was influenced by warm saline bottom water produced in epicontinental seas on Africa and that there was insufficient circulation to homogenize the bottom waters within the South Atlantic basins; however, late Maastrichtian paleotemperatures calculated from isotopic measurements of benthic foraminifera deposited at depths <2000 m in the subtropical South Atlantic are within the range of paleotemperatures estimated for Antarctic intermediate waters, suggesting that the high latitudes were a significant source of intermediate and, possibly, bottom water by the end of the Cretaceous (Barrera and Huber, 1990).

The purpose of this study was to obtain a more continuous, long-term record of middle–Late Cretaceous paleotemperatures using foraminifera that show little or no evidence of diagenetic alteration. DSDP Site 511, from the eastern Falkland Plateau, was chosen for sampling because it yielded an expanded, continuously cored record of Albian–lower Maastrichtian marine sedimentation and because foraminiferal preservation is excellent. During the Cretaceous, Site 511 was up to 10° south of its present latitude of 51°S on eastern Falkland Plateau (Fig. 2). Although there are several stratigraphic gaps in the Albian–lower Maastrichtian sequence at Site 511, results from >200 planktonic and benthic foraminiferal analyses provide significant new insight into the history of changes in surface- and intermediate-water paleotemperatures and vertical oxygen and carbon isotopic gradients, as well as the relative depth distributions of previously unstudied species of planktonic foraminifera.

Two other deep-sea sites were studied to test the reproducibility of isotopic trends observed at Site 511. We analyzed >40 monospecific samples of planktonic and benthic foraminifera from the discontinuously cored Albian–middle Maastrichtian sequence at Site 327 on Falkland Plateau (located ≈100 km northeast of Site 511) and ≈20 monospecific samples of planktonic and benthic foraminifera from the Turonian–Santonian of Site 258 on Naturaliste Plateau in the Indian Ocean (Fig. 2). In addition, five samples of Albian and Campanian planktonic foraminifera from DSDP Site 305 were analyzed to compare tropical Pacific paleotemperatures with the paleotemperature record from the southern South Atlantic and to determine if there are significant differences between the fine-fraction values obtained by Douglas and Savin (1973, 1975) and the separated foraminifera measured in this study.

MATERIAL AND METHODS

Because key marker species used to identify Cretaceous stages and their subdivisions are rare or absent in austral sequences, biostratigraphic resolution tends to be low and uncertainty in age assignments is relatively high at the austral sites. Cross-latitude correlation is achieved by integration of calcareous nannofossil and planktonic foraminifer biostratigraphy with magneto- and strontium isotope stratigraphy wherever possible. The criteria used for chronostratigraphic subdivision at the southern high-latitude sites are outlined in Table 1. Ages reported in this study are based on the revised magnetic polarity and stratigraphic time scale of Gradstein et al. (1994).

Oxygen and carbon isotopic data for DSDP Sites 511, 327, 258, and 305 are presented in Tables 2–5. At each sample level, one to four planktonic foraminifera and one or more benthic species were analyzed. Multispecies planktonic and benthic isotopic values were obtained from intervals where foraminiferal abundance is very low. For all samples, the largest specimens in each species group were selected for analysis to minimize artifacts related to size-dependent changes in isotopic values. For smaller species such as *Hedbergella* sp. 4 (150–200 μm diameter), 70–90 specimens were picked for each isotopic analysis, whereas 10 or fewer specimens of larger species, such as *Globotruncana linneiana* (400–600 μm diameter), were sufficient. Separation of each species into narrowly constrained size fractions was not tenable in this study because of the low abundance of foraminifera in most samples.

Samples were soaked in warm tap water, cleaned in an ultrasonic bath, washed in a 63 μm sieve, and then dried in an oven at 50 °C. Picked foraminiferal splits were reacted in a common acid bath of ortho-phosphoric acid at 90 °C using a VG Isogas autocarbonate preparation system. Isotope ratios of purified CO_2 gas were measured on-line by a VG Prism Series II mass spectrometer. All isotope results are reported in standard δ notation relative to the Pee Dee belemnite standard. Analytical precision, based on routine

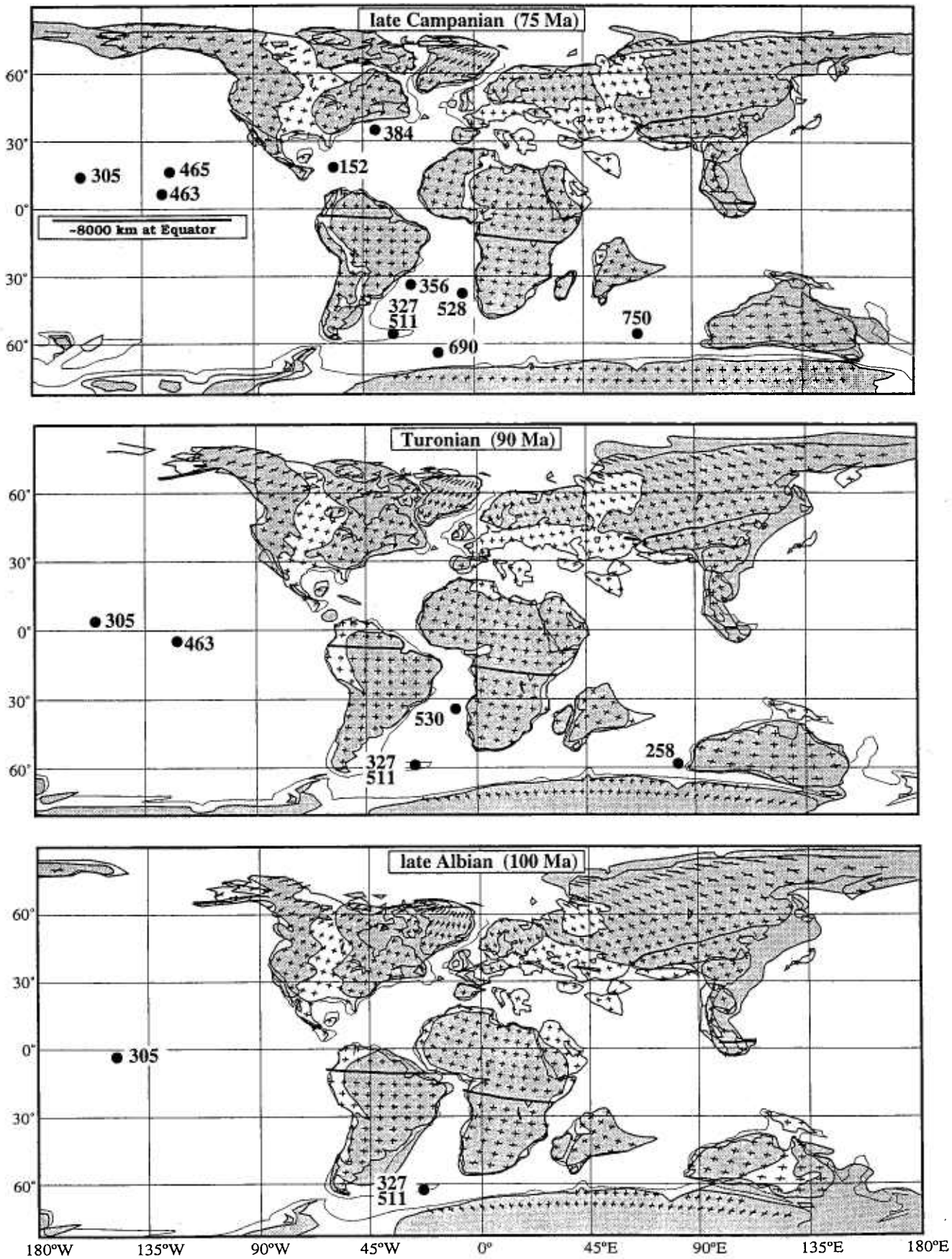

Figure 2. Paleogeographic reconstructions for the late Albian (100 Ma), late Turonian (90 Ma), and late Campanian (75 Ma) based on PGIS[tm] plots overlain with the land-sea distributions of Barron (1987) for the Albian, Turonian, and early Maastrichtian, respectively. Deep Sea Drilling Project and Ocean Drilling Program sites are shown labeled next to the solid circles.

TABLE 2. OXYGEN AND CARBON ISOTOPE VALUES FOR PLANKTONIC AND BENTHIC FORAMINIFERA FROM DEEP SEA DRILLING PROJECT SITE 511

Sample no.	Interval (m)	Depth (mbsf)	Species	$\delta^{18}O$	$\delta^{13}C$
23-1	22–25	195.22	*Heterohelix globulosa*	0.10	0.92
23-1	22–25	195.22	*Archaeoglobigerina australis*	–0.66	2.22
23-1	22–25	195.22	*Gavelinella beccariiformis*	0.40	0.04
23-1	38–41	195.38	*Globigerinelloides prairiehillensis*	–0.10	1.41
24-1	20–23	204.70	*Gavelinella beccariiformis*	–0.17	0.76
24-1	20–23	204.70	*Heterohelix globulosa*	–0.22	1.74
24-1	20–23	204.70	*Archaeoglobigerina australis*	–1.83	2.90
24-1	22–25	204.72	*Globigerinelloides prairiehillensis*	–1.01	2.97
24-2	22–25	206.22	*Heterohelix globulosa*	–0.65	2.03
24-2	22–25	206.22	*Cibicides velascoensis*	0.06	1.28
24-2	22–25	206.22	*Archaeoglobigerina australis*	–1.51	2.90
24-2	22–25	206.22	*Gavelinella beccariiformis*	–0.01	0.83
24-3	20–24	207.70	*Archaeoglobigerina australis*	–1.51	2.79
24-3	20–24	207.70	*Heterohelix globulosa*	–0.13	1.59
24-3	20–24	207.70	*Cibicides velascoensis*	0.02	1.24
24-3	20–24	207.70	*Gavelinella beccariiformis*	–0.11	0.60
24-3	20–24	207.70	*Globigerinelloides prairiehillensis*	–0.92	2.19
24-5	20–24	209.00	*Gavelinella beccariiformis*	–0.17	0.61
24-5	20–24	209.00	*Heterohelix globulosa*	–0.25	1.66
24-5	20–24	209.00	*Cibicides velascoensis*	0.03	1.16
24-5	20–24	209.00	*Archaeoglobigerina australis*	–1.40	2.72
24-5	20–24	209.00	*Globigerinelloides prairiehillensis*	–1.16	2.48
24-7	20–23	209.00	*Globigerinelloides prairiehillensis*	–0.84	2.08
24-7	20–23	209.00	*Archaeoglobigerina australis*	–1.61	2.78
24-7	20–23	209.00	*Cibicides velascoensis*	–0.07	1.06
24-7	20–23	209.00	*Gavelinella beccariiformis*	–0.16	0.68
24-7	20–23	209.00	*Heterohelix globulosa*	–0.46	1.87
28-2	21–25	225.21	*Archaeoglobigerina australis*	–0.61	1.70
28-5	21–25	229.71	*Heterohelix globulosa*	–0.93	1.18
28-6	21–25	231.21	*Charltonina* sp., *Gy. globosa*	–0.51	0.55
29-1	10–13	233.10	*Heterohelix globulosa*	–1.31	1.46
29-CC	42–44	234.92	mixed benthics	–0.90	–0.46
29-CC	42–44	234.92	*Archaeoglobigerina australis*	–1.45	2.45
30-1	23–27	242.73	mixed benthics	–0.54	2.12
30-3	16–20	245.66	*Archaeoglobigerina australis*	–2.63	3.26
30-3	16–20	245.66	*Hedbergella* spp.	–2.29	3.54
30-3	16–20	245.66	*Heterohelix* spp.	–1.48	2.04
30-4	16–20	247.16	*Globigerinelloides alvarezi*	–1.58	2.08
30-5	12–16	248.62	*Osangularia* sp.	–0.56	1.06
31-2.	12–17	253.62	*Archaeoglobigerina australis*	–3.47	3.55
31-2.	12–17	253.62	*Globigerinelloides alvarezi*	–1.75	2.70
31-2.	12–17	253.62	*Gavelinella beccariiformis*	–1.26	0.89
31-4	18–24	256.68	mixed benthics	–0.54	0.79
31-4	18–24	256.68	*Globigerinelloides alvarezi*	–1.80	2.37
31-4	18–24	256.68	*Archaeoglobigerina australis*	–2.84	3.25
31-5	6–11	258.03	*Archaeoglobigerina australis*	–3.40	3.96
31-5	18–21	258.15	mixed benthics	–0.88	–0.11
31-CC	6–8	261.06	*Heterohelix* sp.	–3.41	3.87
31-CC	6–8	261.06	*Hedbergella* spp.	–2.02	3.17
31-CC	6–8	261.06	*Archaeoglobigerina australis*	–2.95	3.64
31-CC	6–8	261.06	mixed benthics	–0.52	1.51
32-1	19–22	261.69	*Archaeoglobigerina australis*	–3.26	2.94
32-1	19–22	261.69	mixed benthics	–0.91	–0.12
32-1	19–22	261.69	*Hedbergella* sp. 4	–2.65	2.86
32-4	22–25	266.22	*Archaeoglobigerina australis*	–3.24	3.40
32-4	22–25	266.22	*Hedbergella* sp. 4	–2.36	3.46
32-6	20–24	269.20	*Archaeoglobigerina australis*	–2.75	3.33
32-6	20–24	269.20	*Hedbergella* sp. 4	–3.07	3.68
32-CC	19–20	270.69	*Gavelinella beccariiformis*	–1.15	0.93
32-CC	19–20	270.69	*Archaeoglobigerina australis*	–2.27	3.18
32-CC	19–20	270.69	*Heterohelix* spp.	–1.30	1.93
33-1	20–24	271.20	*Archaeoglobigerina australis*	–2.49	3.56
33-1	20–24	271.20	*Globotruncana linneiana*	–2.80	3.22
33-1	20–24	271.20	*Heterohelix* spp.	–1.28	2.07
33-1	20–24	271.20	*Gavelinella beccariiformis*	–1.07	1.23
33-1	20–24	271.20	*Hedbergella* sp. 4	–2.34	3.33
33-3	20–24	274.20	*Hedbergella* spp.	–2.50	3.28

TABLE 2. *(Continued)*

Sample no.	Interval (m)	Depth (mbsf)	Species	$\delta^{18}O$	$\delta^{13}C$
33-3	20–24	274.20	*Archaeoglobigenina australis*	–3.46	3.73
33-5	20–24	277.20	*Heterohelix* spp.	–3.01	3.43
33-5	20–24	277.20	*Archaeoglobigenina australis*	–3.12	3.76
33-5	20–24	277.20	*Hedbergella* spp.	–2.50	3.58
33-5	20–24	277.20	*Globotruncana linneiana*	–3.40	2.81
33-6	20–24	278.70	*Globigerinelloides alvarezi*	–1.19	1.74
33-6	20–24	278.70	*Archaeoglobigerina australis*	–2.27	3.08
33-CC	16–19	280.16	*Archaeoglobigerina australis*	–3.56	3.38
34-1	20–24	280.70	*Hedbergella* sp. 4	–3.24	3.70
34-1	20–24	280.70	*Archaeoglobigerina cretacea*	–2.54	2.36
34-3	14–19	283.64	*Heterohelix globulosa*	–3.44	3.43
34-3	14–19	283.64	*Archaeoglobigerina cretacea*	–2.53	2.76
34-3	20–24	283.70	*Globorotaloides nitidus*	–0.77	0.87
34-4	20–24	285.20	*Archaeoglobigerina australis*	–2.22	3.86
34-4	22–26	285.22	*Hedbergella* sp. 4	–3.31	3.27
34-7	20–24	289.70	*Archaeoglobigenina cretacea*	–2.51	2.57
34-7	20–24	289.70	mixed benthics	–0.79	0.90
34-7	20–24	289.70	*Hedbergella* sp. 4	–2.67	3.30
35-1	20–24	290.20	*Archaeoglobigenina cretacea*	–3.03	2.97
35-1	20–24	290.20	*Hedbergella* sp. 4	–2.78	3.14
35-2	20–24	291.70	*Hedbergella* sp. 4	–2.85	3.35
35-2	20–24	291.70	*Archaeoglobigerina cretacea*	–2.64	2.94
35-CC	10–12	293.10	*Archeoglobigerina cretacea*	–2.40	2.98
36-1	24–28	299.74	*Archaeoglobigerina cretacea*	–1.71	2.14
36-1	24–28	299.74	mixed benthics	–0.75	0.26
36-1	24–28	299.74	*Hedbergella* sp. 4	–3.56	3.78
36-1	24–28	299.74	*Heterohelix globulosa*	–3.95	3.49
36-2	24–28	301.24	*Globotruncana bulloides*	–2.39	2.41
36-2	24–28	301.24	*Marginotruncana marginata*	–2.23	2.05
36-2	24–28	301.24	*Heterohelix globulosa*	–3.89	3.29
36-2	24–28	301.24	mixed benthics	–1.10	0.72
36-3	24–28	302.74	*Hedbergella* sp. 4	–3.19	3.29
36-3	24–28	302.74	*Archaeoglobigenina cretacea*	–1.42	1.90
36-4	23–27	304.23	*Hedbergella* sp. 4	–3.44	3.72
36-4	23–27	304.23	*Archaeoglobigenina cretacea*	–3.33	2.23
36-5	23–27	305.73	*Gavelinella* sp.	–1.02	0.15
36-5	23–27	305.73	*Charltonina* sp.	–0.97	0.75
36-5	23–27	305.73	*Gyroidina globosa*	–0.30	1.43
36-5	33–35	305.83	*Archaeoglobigenina cretacea*	–1.98	2.50
36-6	23–27	307.23	*Archaeoglobigenina cretacea*	–1.75	2.23
36-6	23–27	307.23	*Heterohelix* spp.	–0.97	1.48
36-6	23–27	307.23	*Heterohelix globulosa*	–3.71	3.70
37-1	23–27	309.23	mixed benthics	–0.82	0.20
37-1	23–27	309.23	*Archaeoglobigerina cretacea*	–2.23	2.27
37-1	23–27	309.23	*Hedbergella* sp. 4	–2.74	2.81
37-2	23–27	310.73	*Archaeoglobigerina cretacea*	–2.24	2.14
38-1	24–28	318.74	*Archaeoglobigerina cretacea*	–2.62	2.90
38-2	24–28	320.24	*Archaeoglobigerina cretacea*	–3.53	3.24
38-4	24–28	323.24	*Globotruncana bulloides*	–3.72	3.33
38-4	24–28	323.24	mixed benthics	–0.99	1.05
38-6	13–17	326.13	*Gyroidinoides nitidus*	–0.86	–0.04
38-6	20–23	326.20	*Marginotruncana marginata*	–2.16	2.37
38-6	20–23	326.20	*Heterohelix globulosa*	–3.49	3.30
39-3	20–24	331.20	*Globotruncana bulloides*	–3.40	3.02
39-3	20–24	331.20	mixed benthics	–0.73	0.26
39-CC	8–11	334.08	*Globotruncana bulloides*	–3.27	3.27
39-CC	8–11	334.08	*Archaeoglobigerina australis*	–3.62	3.70
39-CC	8–11	334.08	*Heterohelix globulosa*	–1.23	1.65
40-1	16–20	337.66	mixed benthic	–0.77	0.01
40-1	21–23	337.71	*Globotruncana bulloides*	–3.36	2.47
40-1	21–23	337.71	*Globigerinelloides alvarezi*	–1.53	1.87
40-1	21–23	337.71	*Heterohelix* spp.	–1.53	1.56
40-4	26–29	342.26	*Globigerinelloides alvarezi*	–2.10	1.98
40-4	26–29	342.26	*Heterohelix globulosa*	–1.45	1.59
40-5	16–20	343.66	*Globotruncana bulloides*	–3.37	2.34
40-5	22–25	343.72	*Globorotaloides multisepta*	–1.09	0.66
40-6	20–23	345.20	*Heterohelix globulosa*	–1.28	1.90

TABLE 2. *(Continued)*

Sample no.	Interval (m)	Depth (mbsf)	Species	$\delta^{18}O$	$\delta^{13}C$
41-3	18–21	350.18	*Heterohelix globulosa*	−1.03	1.78
41-3	18–21	350.18	*Globotruncana bulloides*	−2.29	1.37
41-3	18–21	350.18	*Globigerinelloides alvarezi*	−0.62	2.45
41-3	18–21	350.18	*Globorotaloides* spp.	−1.07	1.08
42-4	21–23	381.21	*Heterohelix globulosa*	−1.80	2.52
42-4	21–23	361.21	*Globigerinelloides alvarezi*	−1.97	2.86
42-4	21–23	361.21	*Archaeoglobigerina australis*	−2.57	2.67
43-1	20–23	366.20	*Charltonina* sp.	−1.26	0.87
43-1	20–23	366.20	*Gyoidinoides* sp.	−0.93	0.60
43-1	20–23	366.20	*Heterohelix globulosa*	−1.96	2.13
43-2	23–26	367.73	*Heterohelix globulosa*	−1.56	2.34
43-2	23–26	367.73	*Archaeoglobigerina bosquensis*	−1.98	3.01
43-5	19–22	372.19	*Archaeogloibgerina cretacea*	−3.58	3.19
43-5	19–22	372.19	*Heterohelix globulosa*	−2.34	2.71
43-5	19–22	372.19	mixed benthics	−0.94	1.16
44-1	24–26	375.74	*Heterohelix globulosa*	−1.09	−0.94
44-1	24–28	375.74	*Globigerinelloides alvarezi*	−0.13	2.60
44-3	20–23	378.70	*Globorotaloides* sp.	−1.19	1.20
45-1	90–92	385.90	*Heterohelix globulosa*	−2.03	2.06
46-1	10–15	394.60	*Gyroidinoides nitidus*	−1.00	−0.46
46-1	10–15	394.80	mixed benthics	−1.16	−0.42
46-1	21–24	394.71	*Archaeoglobigerina bosquensis*	−3.45	2.50
46-3	13–18	397.63	*Gyroidlna?* sp.	−0.94	−0.57
46-3	13–18	397.63	mixed benthics	−1.12	−0.45
46-CC	5–7	400.55	*Archaeoglobigerina bosquensis*	−3.02	2.75
46-CC	5–7	400.55	*Gyrodinoides nitidus*	−1.37	0.19
47-3	23–25	407.23	*Whiteinella baltica*	−2.52	1.78
47-3	23–25	407.23	mixed benthic	−1.46	0.01
47-4	23–25	408.73	*Whiteinella baltica*	−2.82	1.16
47-4	23–25	408.73	*Globotruncana bulloides*	−3.53	1.39
47-5	18–20	410.18	*Archaeoglobigerina bosquensis*	−3.88	1.94
47-5	18–20	410.18	*Whiteinella baltica*	−3.19	1.71
47-6	18–20	411.68	*Globotruncana bulloides*	−4.39	1.43
47-6	18–20	411.68	*Archaeoglobigerina bosquensis*	−4.35	1.63
47-6	18–20	411.68	*Whiteinella baltica*	−3.34	1.54
48-1	14–18	413.64	mixed benthics	−1.53	0.17
48-1	24–27	413.74	*Whiteinella baltica*	−2.31	0.81
48-1	24–27	413.74	*Praeglobotruncana stephani*	−2.04	0.31
49-5	24–26	429.24	*Whiteinella brittonensis*	−1.91	2.15
49-5	24–26	429.24	*Hedbergella* sp.1	−1.42	1.89
49-5$_a$	24–26	429.24	*Gavelinella* sp.	−0.38	0.94
49-6	24–26	430.74	*Gyroidina globosa*	−0.33	1.38
49-6	24–26	430.74	*Hedbergella* spp.	−1.09	2.30
50-3	26–28	435.76	*Gyroidina globosa*	−0.24	1.39
50-3	26–28	435.76	*Hedbergella* spp.	−0.71	2.37
51-3	21–23	445.21	*Gyroidina globosa*	−0.42	1.49
51-3	21–23	445.21	*Hedbergella* spp.	−1.19	2.45
52-3	25–27	454.75	*Hedbergella* spp.	−1.30	2.49
52-3	25–27	454.75	*Gyroidina globosa*	−0.12	1.32
53-1	25–27	461.25	*Hedbergella* spp.	−0.99	2.45
53-1	25–27	461.25	*Gyroidina globosa*	0.30	1.52
54-3	22–24	473.72	*Gyroidina globosa*	0.17	1.02
54-3	22–24	473.72	*Hedbergella* spp.	−0.77	2.44
54-3	22–24	473.72	*Osangularia schloenbachi*	0.53	1.48
55-3	24–26	483.24	*Gyroidina globosa*	−1.73	0.04
55-3	24–26	483.24	*Gavelinella* sp.	0.44	1.37
55-3	24–26	483.24	*Gyroidina globosa*	−1.10	0.52
58-5	22–25	495.63	*Gyroidina globosa*	0.50	2.15
56-5	22–25	495.63	*Gavelinella* sp.	0.30	2.30

Note: The sample interval in each core section and depth in meters below sea floor (mbsf) are listed for each sample.

TABLE 3. OXYGEN AND CARBON ISOTOPE VALUES FOR PLANKTONIC AND BENTHIC FORAMINIFERA FROM DEEP SEA DRILLING PROJECT HOLE 327A

Sample no.	Interval (m)	Depth (mbsf)	Species	$\delta^{18}O$	$\delta^{13}C$
10-2	136–138	92.00	*Archaeoglobigerina australis*	−0.76	2.50
10-2	136–138	92.00	*Gavelinella beccariiformis*	0.55	−0.45
10-2	136–138	92.00	*Heterohelix planata*	0.35	1.06
10-3	22–24	92.72	*Archaeoglobigerina australis*	−0.54	2.44
10-3	22–24	92.72	*Heterohelix planata*	0.42	0.93
10-CC		94.50	*Archaeoglobigerina australis*	−0.56	2.50
10-CC		94.50	*Gavelinella beccariiformis*	0.43	−0.16
10-CC		94.50	*Heterohelix planata*	0.23	1.11
11-1	14–16	99.14	*Archaeoglobigerina australis*	−0.41	2.13
11-1	14–16	99.14	*Gavelinella beccariiformis*	0.35	−0.38
11-1	14–16	99.14	*Heterohelix planata*	0.52	0.95
11-2	108–110	101.58	*Archaeoglobigerina australis*	−0.69	2.21
11-2	108–110	101.58	*Gavelinella beccariiformis*	0.13	−0.52
11-2	108–110	101.58	*Heterohelix planata*	0.34	0.90
12-1	64–66	109.14	*Archaeoglibigerina australis*	−0.94	2.34
12-1	64–68	109.14	*Heterohelix planata*	0.41	0.92
12-2	84–86	110.84	*Archaeoglobigerina australis*	−0.64	2.28
12-2	84–86	110.84	*Gavelinella beccariiformis*	0.15	−0.13
12-2	84–86	110.84	*Heterohelix planata*	0.33	0.94
12-3	86–88	112.38	*Archaeoglobigerina australis*	−0.91	2.37
12-3	86–88	112.36	*Gavelinella beccariiformis*	0.28	−0.14
12-3	86–88	112.38	*Heterohelix planata*	0.34	0.94
12-4	24–26	113.24	*Archaeoglobigerina australis*	−0.84	2.20
12-4	24–26	113.24	*Gavelinella beccariiformis*	0.28	−0.20
12-4	24–26	113.24	*Heterohelix planata*	0.48	0.96
13-1	143–145	138.43	*Archaeoglobigerina australis*	−1.25	2.74
13-1	143–145	138.43	*Heterohelix planata*	0.17	1.20
13-2	64–66	139.14	*Archaeoglobigerina australis*	−0.71	2.28
13-2	64–66	139.14	*Gavelinella beccariiformis*	−0.14	0.48
13-2	64–66	139.14	*Heterohelix planata*	0.17	1.34
14-1	121–123	147.71	*Heterohelix globulosa*	−0.66	2.37
14-1	121–123	147.71	*Gyroidina globosa*	−0.53	1.56
14-1	121–123	147.71	*Aragonia materna*	−0.56	1.59
14-6	67–69	154.67	*Angulogavelinella* sp.	−0.16	1.72
14-6	67–69	154.67	*Gavelinella* sp.	−0.50	1.82
15-2	13–15	176.63	*Gavelinella* sp.	−0.35	1.51
15-2	13–15	176.63	*Cibicides* sp.	−0.55	1.63
15-2	13–15	176.63	*Hedbergella delrioensis*	−1.26	2.30

Note: The sample interval in each core section and depth in meters below sea floor (mbsf) are listed for each sample.

analysis of an internal carbonate standard (Carrara Marble), was better than 0.1% for $\delta^{18}O$ and $\delta^{13}C$.

Strontium isotope values (Table 6) were obtained from laboratories at the University of Florida and the University of North Carolina using foraminifer samples (and bivalve fragments when foraminifera were too rare) that ranged from 1 to 11 mg in size. At the University of Florida laboratory, the 2–8 mg samples were dissolved in 0.25 N HCl, dried, and then dissolved in 250 μl of 2.5N HCl. After centrifuging, the 250 μl sample was loaded onto standard Dowex 50 × 12 cation exchange columns and eluted in 2.5 N HCl. The strontium fraction (5 ml) was collected and evaporated until dry. Strontium was then loaded on a single oxidized Ta filament. Isotopic ratios were measured on a VG Instruments 354 triple collector mass spectrometer in the dynamic mode, with mass fractionation normalized to a $^{86}Sr/^{88}Sr$ ratio of 0.1194. For values reported here, 200 ratios were collected on each sample, which resulted in a "within-run" precision of better than 1×10^{-5} for most samples. Recent $^{87}Sr/^{86}Sr$ analyses of Sr carbonate standard SRM 987 yielded a value of 0.710 248 ± 3 (2σ). Long-term analyses of SRM 987 yielded an average $^{87}Sr/^{86}Sr$ value of 0.710 235. Internal precision for Sr carbonate runs was typically 0.0006%–0.0009% standard error. At the University of North Carolina laboratory, milligram to submilligram quantities of powdered carbonate were dissolved in 15 mL Savillex PFA vials using 250 = B5L of 2× distilled 5 N HNO_3 in a class 100 filtered air environmental hood. Sr was separated from matrix using EiChrom SrSpec resin, a crown-ether Sr-selective resin (50–100 = B5m diameter) loaded into either the tip of a 10 mL BioRad polypropylene column or into a Teflon column (10 × 4 mm) with reservoir. Total resin volume was ≈50 = B5L. SrSpec resin

TABLE 4. OXYGEN AND CARBON ISOTOPE VALUES FOR PLANKTONIC AND BENTHIC FORAMINIFERA FROM DEEP SEA DRILLING PROJECT SITE 258

Sample no.	Interval (m)	Depth (mbsf)	Species	$\delta^{18}O$	$\delta^{13}C$
Site 258					
5-3	108–111	127.58	*Angulogavelinella* sp.	–0.58	1.71
5-3	108–111	127.58	*Archaeoglobigerina bosquensis*	–1.75	3.58
5-3	108–111	127.58	*Heterohelix globulosa*	–0.97	3.22
5-3	108–111	127.58	*Globotruncana linneiana*	–1.25	2.81
6-3	110–113	146.60	*Archaeoglobigerina bosquensis*	–2.28	2.93
6-3	110–113	146.60	*Globotruncana linneiana*	–2.08	2.62
6-3	110–113	146.60	*Angulogavelinella* sp.	–1.09	1.54
7-2	110–112	154.60	*Heterohelix globulosa*	–1.51	2.75
7-2	110–112	154.60	*Globotruncana linneiana*	–1.99	2.82
7-2	110–112	154.60	*Archaeoglobigerina bosquensis*	–2.24	3.20
7-2	110–112	154.60	*Angulogavelinella* sp.	–0.86	1.82
9-1	38–41	180.88	*Archaeoglobigerina bosquensis*	–2.01	2.91
9-1	38–41	180.88	*Angulogavelinella* sp.	–0.95	1.03
9-1	38–41	180.88	*Globotruncana linneiana*	–2.48	2.97
10-2	53–54	201.53	*Archaeoglobigerina bosquensis*	–2.82	2.89
10-2	53–54	201.53	*Angulogavelinella* sp.	–1.27	1.30
10-2	53–59	201.53	*Globotruncana linneiana*	–2.54	2.74
11-3	76–80	219.26	*Angulogavelinella* sp.	–1.14	1.95
14-1	83–86	263.83	*Angulogavelinella* sp.	–0.80	1.58
14-1	83–86	283.83	*Hedbergella delrioensis*	–1.85	3.38
Hole 258A					
9-3	130–133	118.30	*Heterohelix globulosa*	–0.57	2.37
9-3	130–133	118.30	*Archaeoglobigerina bosquensis*	–1.61	3.10
9-3	130–133	118.30	*Angulogavelinella* sp.	–0.46	1.33
9-3	130–133	118.30	*Globotruncana linneiana*	–1.45	2.59

Note: The sample interval in each core section and depth in meters below sea floor (mbsf) are listed for each sample.

must be presoaked and flushed with H_2O to remove Sr present from the resin manufacturing process. Resin is further cleaned in the column with repeated washes of deionized H_2O and conditioned with 5 N HNO_3. Resin was used once for sample elution and discarded. The dissolved sample was loaded and washed in 750 mL of 5 N HNO_3, then Sr was eluted with 1 mL of H_2O. Total procedural blanks for Sr were typically 60 picograms (pg). Sr loading blanks were <3 pg. Sr was ionized on degassed Ta filaments, and isotopic ratios were measured on a VG Sector 54 thermal ionization mass spectrometer at the University of North Carolina-Chapel Hill in quintuple-collector dynamic mode, using the internal ratio $^{86}Sr/^{88}Sr$ = 3D 0.1194 to correct for mass fractionation. Recent $^{87}Sr/^{86}Sr$ analyses of Sr carbonate standard SRM 987 yielded a value of 0.710 245 ± 18 (2σ). Long term analyses (≈24 months) of SRM 987 yielded an average $^{87}Sr/^{86}Sr$ value of 0.710 242. Internal precision for Sr carbonate runs is typically 0.0006%–0.0009% standard error, based on 100 dynamic cycles of data collection and a 1 mg carbonate sample. To minimize interrun variability and standardize values from both laboratories, all data were normalized to a constant SRM-987 = 0.710 242.

TABLE 5. OXYGEN AND CARBON ISOTOPE VALUES FOR EARLY CAMPANIAN AND LATE ALBIAN PLANKTONIC AND BENTHIC FORAMINIFERA FROM DEEP SEA DRILLING PROJECT SITE 305

Sample no.	Interval (m)	Depth (mbsf)	Species	$\delta^{18}O$	$\delta^{13}C$
25-2	80–84	225.80	*Globotruncana linneiana*	–1.03	2.40
25-2	80–84	225.80	*Globotruncanita stuartiformis*	–0.93	2.22
26-4	100–104	233.00	*Globotruncanita stuartiformis*	–1.06	2.10
26-4	100–104	233.00	*Globotruncana linneiana*	–1.37	2.32
41-CC		373.50	*Hedbergella delrioensis*	–3.25	1.61
41-CC		373.50	*Rotalipora greenhornensis*	–2.70	1.34

Note: The sample interval in each core section and depth in meters below sea floor (mbsf) are listed for each sample.

TABLE 8. STRONTIUM ISOTOPE DATA OF SOME BENTHIC AND PLANKTONIC FORAMINIFERAL SAMPLES FROM THE APTIAN–LOWER MAASTRICHTIAN OF DEEP SEA DRILLING PROJECT SITE 511

Sample no.	Interval (m)	Depth (mbsf)	$^{87}Sr/^{86}Sr$
23-1	38–41	195.38	0.707 739 ± 6*
24-1	20–25	204.70	0.707 675 ± 6*
24-3	20–24	207.70	0.707 691 ± 6*
24-5	20–25	209.00	0.707 702 ± 8*
24-7	20–23	209.00	0.707 673 ± 8*
28-8	23–29	231.23	0.707 423 ± 6*
30-4	23–25	247.23	0.707 354 ± 6*
31-5	33–35	258.33	0.707 456 ± 7*
33-4	78–80	278.28	0.707 458 ± 9*
33-6	23–29	278.78	0.707 436 ± 5
34-4	26–32	285.29	0.707 431 ± 4
36-2	24–28	301.26	0.707 422 ± 4
36-5	27–33	305.80	0.707 448 ± 4
40-1	21–23	337.72	0.707 419 ± 5
41-3	12–21	350.17	0.707 412 ± 4
42-2	25–31	358.28	0.707 412 ± 5
42-5	27–29	362.77	0.707 363 ± 5*
43-4	23–24	370.73	0.707 356 ± 4
45-1	27–28	385.27	0.707 320 ± 7*†
47-3	25–31	407.28	0.707 356 ± 6*
47-6	38–40	411.88	0.707 304 ± 7*†
47-6	38–40	411.88	0.707 349 ± 9*
48-1	18–24	413.71	0.707 413 ± 4
49-5	24–26	429.25	0.707 365 ± 5†
50-1	17–19	432.68	0.707 371 ± 4†
50-1	29–33	432.81	0.707 381 ± 5†
51-1	22–24	442.23	0.707 435 ± 5†
51-5	24–26	448.25	0.707 400 ± 5†
52-1	20–22	451.71	0.707 433 ± 8†
52-3	9–12	454.61	0.707 418 ± 5†
52-5	27–29	457.78	0.707 379 ± 4†
52-5	27–29	457.78	0.707 380 ± 4†
52-7	8–10	460.59	0.707 413 ± 6†
53-1	25–27	461.26	0.707 386 ± 4†
53-5	27–29	467.28	0.707 384 ± 4†
54-3	22–24	473.73	0.707 314 ± 6†
55-1	24–26	480.25	0.707 274 ± 5§
55-5	24–26	486.24	0.707 281 ± 6*†
56-5	1–3	495.52	0.707 355 ± 5§

Note: Values are normalized to NBS 987=71042 ± 10 (1σ), and the standard error is expressed for each sample run. Data are from the laboratory at the University of Florida unless otherwise indicated.
*Samples run at the University of North Carolina.
†Bivalve shells.
§Foraminifera and bivalve shells.

Paleocoordinates of DSDP and ODP sites (Fig. 2) were determined from the commercial rotation program Paleogeographic Information System™ (PGIS) of Scotese and Zonenshein (PALEOMAP Project, 1992, unpubl. data).

STRATIGRAPHY OF THE STUDIED SECTIONS

DSDP Site 511, Falkland Plateau

Site 511 is located in the Falkland Plateau Basin at lat 51°00′S and long 47°58′W at a water depth of 2589 m. Paleogeographic reconstructions indicate that this site was at ≈61°S during the late Albian and migrated to ≈56°S by the end of the Campanian (Fig. 2).

Open marine conditions were probably established at the site by the early Albian. After final separation of the Falkland Plateau from South Africa, the basin rapidly subsided and reached bathyal depths sometime during the late Albian–Cenomanian (Basov and Krasheninnikov, 1983). Terrigenous source terrains were in southern South America and may have also existed south of Falkland Plateau along a convergent margin between the Malvinas plate and the South American plate (LaBrecque, 1986; Cielsielski, Kristoffersen et al., 1988, Chapter 5, their Figs. 8, 9, 34). The shallow burial depth and high clay percentage in most of the Albian–lower Maastrichtian sequence account for the excellent preservation of Cretaceous calcareous microfossils at Site 511.

Mesozoic sediments recovered at Site 511 range from the Upper Jurassic through lower Maastrichtian, but well-preserved foraminifera are confined to a 314 m thick Albian–lower Maastrichtian interval that spans from 195 to 499 m below the sea floor (mbsf). Core recovery within this interval averaged 70%. The lithostratigraphy of the sequence was originally described in Ludwig et al. (1983) and is depicted in Figure 3, and the biostratigraphy is based on calcareous nannoplankton (Wise, 1983; Wind and Wise, 1983) and planktonic foraminifera (Krasheninnikov and Basov, 1983), with modifications by Huber (1992) and Bralower (1992). Foraminifera are abundant throughout the upper Campanian–lower Maastrichtian and Albian chalk sections, but their abundance and the planktonic:benthic foraminiferal ratios vary considerably within the sequence, ranging from nearly 100% in the calcareous chalk to <1% in some zeolitic clay samples (Fig. 3). The percent carbonate in the cores is also variable, ranging from ≈65% in the calcareous chalk to ≈1% in the zeolitic clay. Dilution by terrigenous clays probably accounts for most of the variability in carbonate content, although a shallowing of the foraminiferal lysocline has been attributed to a loss of the calcareous microfossil record during the late Cenomanian and middle Campanian (Wise, 1983; Basov and Krasheninnikov, 1983).

New strontium isotope data obtained from Site 511 (Fig. 4) corroborate most of the biostratigraphic age assignments that are outlined in Table 1. Figure 3 shows generally good correspondence between the $^{87}Sr/^{86}Sr$ values obtained from core 511-56 through -23 and a best-fit seawater strontium isotope curve compiled from published sources by Jones et al. (1994) and Sugarman et al. (1995). Key tie points between the Site 511 $^{87}Sr/^{86}Sr$ values and the composite curve include (1) values ranging from 0.707 28 to 0.707 36 in cores 511-56 through -55 (500–480 mbsf), consistent with an Aptian–early Albian age; (2) values ranging from 0.707 31 to 0.707 36 in cores 511-47 through -45 (412–385 mbsf), consistent with a late Turonian–early Coniacian age; (3) values ranging from 0.707 68 to 0.707 70 in core 511-24 (209–204 mbsf), consistent with a late Campanian age; and (4) a value of 0.707 75 from core 511-23 (195 mbsf), consistent with an early Maastrichtian age. The most significant discrepancy between the composite and Site 511 strontium isotope curves is in the early Campanian. The composite curve indicates steadily increasing $^{87}Sr/^{86}Sr$ values in the early Campanian, whereas the Site 511 results show a plateau of $^{87}Sr/^{86}Sr$ values for this assigned time. This and other discrepancies between the two curves may be the result of one or a combination of factors at Site 511, including significant variations in sedimentation rates, the presence of additional hiatuses, incorrect biostratigraphic age assignments, and/or diagenesis. On the other hand, the Site 511 $^{87}Sr/^{86}Sr$ record may include variations in seawater strontium isotopic ratios that have not been identified elsewhere. More detailed analysis of the Site 511 biostratigraphy and strontium isotope stratigraphy, and additional strontium isotope data from well-dated Upper Cretaceous sequences elsewhere, will help to resolve the uncertain age assignments at Site 511.

DSDP Hole 327A, Falkland Plateau

This hole is also located in the Falkland Plateau Basin (lat 50°52′S, long 46°47′W), ≈10 km northeast of Site 511 in a water depth of 2410 m. Although >380 m of Cretaceous sediment was drilled in this hole, most of the sequence was cored discontinuously, and core recovery averaged only 50%. The upper Albian–lower Maastrichtian sediments examined in this study were buried at shallow depth, from 90 to 177 mbsf (Fig. 5). The paleobathymetric history of Site 327 is similar to that of Site 511, whereby sedimentation was above the shelf/slope break during most of the Albian, and the basin rapidly subsided to bathyal depths by the end of the Albian (Sliter, 1977). Corroded foraminiferal tests and low planktonic:benthic ratios in core 327A-14 suggest deposition below the foraminiferal lysocline during the Cenomanian and Santonian, while noncorroded foraminifera and high planktonic:benthic ratios indicate deposition above the foraminiferal lysocline in a lower bathyal environment during the Campanian and early Maastrichtian (Sliter, 1977).

The upper Albian–lower Maastrichtian litho- and biostratigraphy for hole 327A are summarized in Figure 5. Age assignments are based on the calcareous nannoplankton and planktonic foraminifer biostratigraphies of Sliter (1977) and Wise and Wind (1977), with subsequent modifications (Wind and Wise, 1983; Huber, 1992). Major disconformities span the upper Maastrichtian and occur between the Cenomanian and Santonian and the Santonian and Campanian intervals.

DSDP Site 258, Southeast Indian Ocean

This site is located off southwest Australia on Naturaliste Plateau (lat 33°48′S, long 112°42′E) at 2793 m water depth. Paleogeographic reconstructions of the southeast Indian Ocean indicate that the continental margins of Australia and Antarctica were joined during the Mesozoic until slow spreading began to separate these continents during the Cenomanian (Veevers, 1986, 1987). Because this spreading initially pivoted about southeast Australia, Site 258 remained located at ≈58°S throughout Late Cretaceous time (Fig. 2).

Drilling at Site 258 penetrated a 411-m-thick middle Albian–Santonian sequence, but the Cretaceous record is very incomplete because of discontinuous coring, poor core recovery (≈40%), and a disconformity that separates Santonian from upper Miocene sediments (Davies et al., 1974; Fig. 6). The shipboard biostratigraphies for planktonic foraminifera and nannofossils were the responsibility of Herb (1974) and Thierstein (1974), respectively. The Upper Cretaceous sediments were deposited at bathyal depths and are presently buried under 123 m of sediment. Foraminiferal abundance is high in the Coniacian–Santonian interval, with high planktonic:benthic ratios in cores 258-5 through -10, and low planktonic:benthic ratios in cores 258-11 and -12, but foraminifera are sparse and very low in diversity in the Turonian and older interval.

About 10 m of coccolith ooze of Santonian age was penetrated in nearby hole 258A. Correlation of planktonic foraminifera and calcareous nannofossils indicate that core 9 in Hole 258A, which was

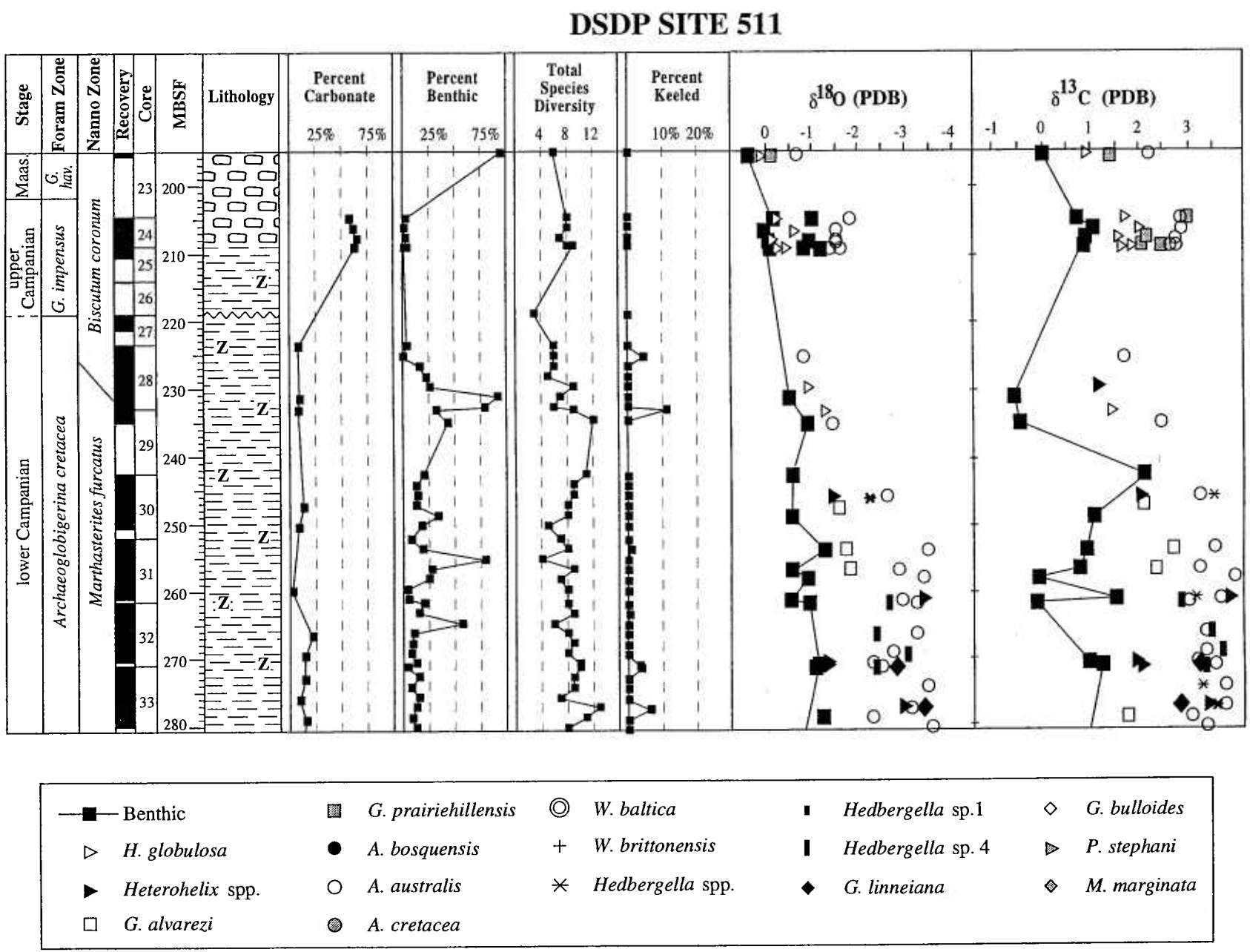

Figure 3. (*See caption on page 1174.*)

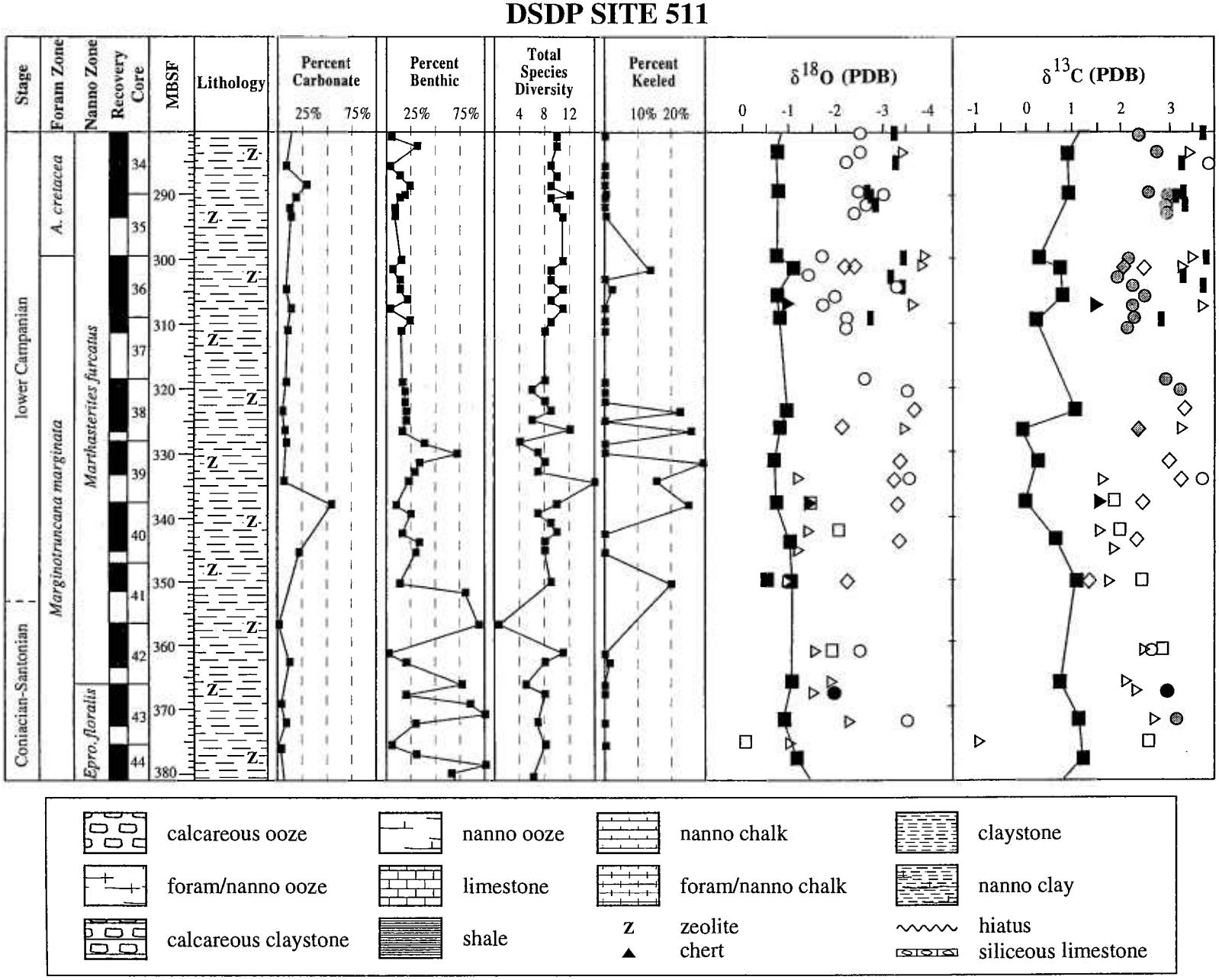

Figure 3. (*Continued.*) (*See caption on page 1174.*)

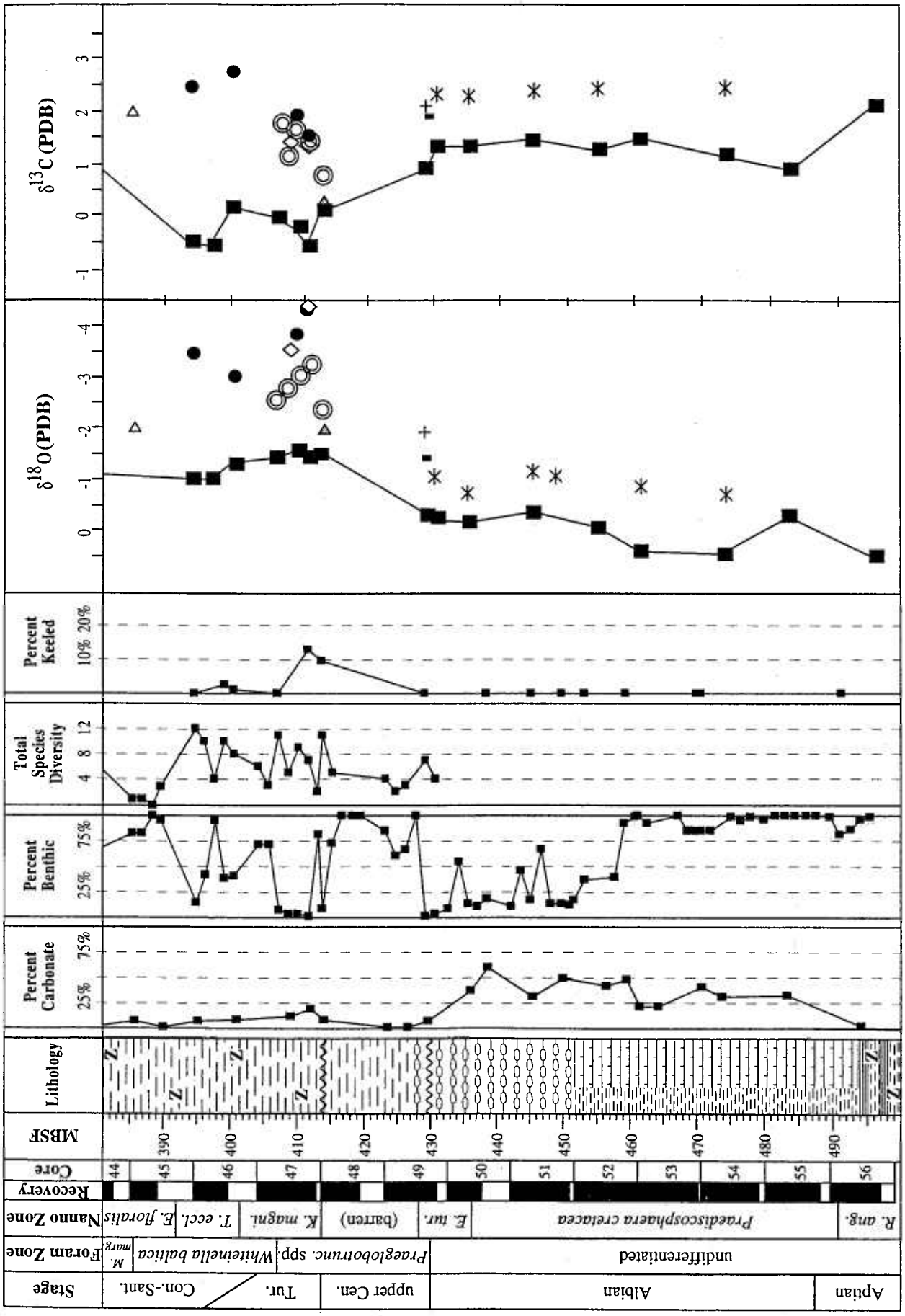

Figure 3. (*Continued.*) Oxygen and carbon isotopic plots for >200 samples of benthic and planktonic foraminifera from Deep Sea Drilling Project Site 511 relative to the Cretaceous stages, planktonic foraminiferal and calcareous nannoplankton biostratigraphy, core recovery, lithology, and percent carbonate. Percent benthic foraminifera, total planktonic foraminifer species diversity, and percent keeled planktonic species also are shown. Samples with more than one isotopic analysis of benthic species are shown as averaged values. Isotopic data are presented in Table 2.

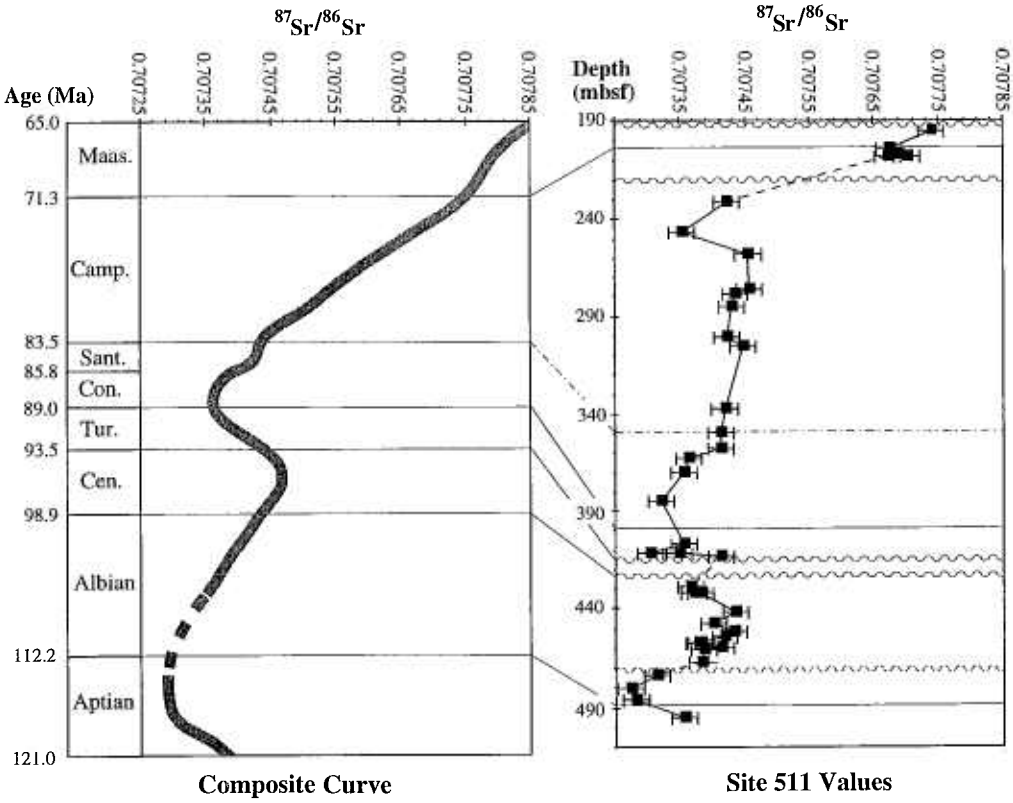

Figure 4. Composite strontium isotope seawater curve correlated with strontium isotopic values obtained from Deep Sea Drilling Project Site 511. The composite curve is based on a compilation of published best estimates from sources discussed in Jones et al. (1994, Fig. 5), adjusted to the Gradstein et al. (1994) time scale, with the addition of $^{87}Sr/^{86}Sr$ values from McArthur et al. (1993, 1994) and Sugarman et al. (1995) for the Maastrichtian. All values are normalized to NBS 987 = 710242. The standard error (2σ) of the Site 511 samples is 2×10^{-5}. Stippled, dashed line in the composite curve represents an interval lacking $^{87}Sr/^{86}Sr$ data; dashed lines in the Site 511 curve cross interval with a disconformity; wavy horizontal lines represent disconformities; broken wavy line represents disconformity inferred from strontium isotope data; and dash-dot horizontal line represents uncertain Santonian-Campanian age boundary.

included in this study (Table 4), is about the equivalent of core 5 from Site 258 (Davies et al., 1974). Keeled planktonic species are significantly more abundant, and total planktonic species diversity is higher in the Coniacian–Santonian from holes 258 and 258A than in coeval assemblages from Falkland Plateau.

MICROFOSSIL PRESERVATION

Diagenetic alteration of the original isotopic composition of biogenic calcite is the biggest problem affecting isotopic paleotemperature studies of Cretaceous deep-sea sediments. Dissolution and reprecipitation of calcite affect isotopic ratios because the physical and chemical properties of pore fluids are different from the seawater in which the microfossils grew. In foraminifera, shell recrystallization may result in encrustation of the chamber walls or replacement of the original wall calcite. Encrustation can be identified using a binocular microscope or scanning electron microscope to detect the presence of calcite rhombs on the inside or outside surface of chamber walls, which give a sugary appearance to tests observed under a light microscope, and/or the infilling of pores or apertures by blocky calcite. Replacement can be recognized with a scanning electron microscope by the absence of microlayering, absence of radial calcite prisms, and/or an irregular, blocky appearance of the shell wall in cross-sectional view.

Diagenetic recrystallization is evident in foraminifera from many Cretaceous marine sequences. Schrag et al. (1992) have concluded that diagenetic alteration of planktonic foraminifera from low latitudes leads to higher $\delta^{18}O$ values in the secondary calcite and an underestimation of deep- and surface-water temperatures. These authors also have determined that diagenetic effects on foraminifera from high latitudes have caused a negative shift in the $\delta^{18}O$ values of high-latitude foraminifera, leading to an overestimation of deep- and surface-water temperatures. The $\delta^{13}C$ composition of foraminifera in deep-sea sediments with low organic carbon is generally less susceptible to dissolution-reprecipitation diagenesis because the noncarbonate carbon pool in sediment pore waters is usually small.

We microscopically examined representative foraminifera from each site to estimate the extent of recrystallization (Figs. 7 and 8). The shells of planktonic and benthic foraminifera from the lower Campanian of Site 511 (Fig. 7a) show excellent preservation with clean inner chamber surfaces and pore interiors and observable microlayering. This is typical of all foraminifera found in the zeolitic claystone from the Turonian–Santonian interval through the upper

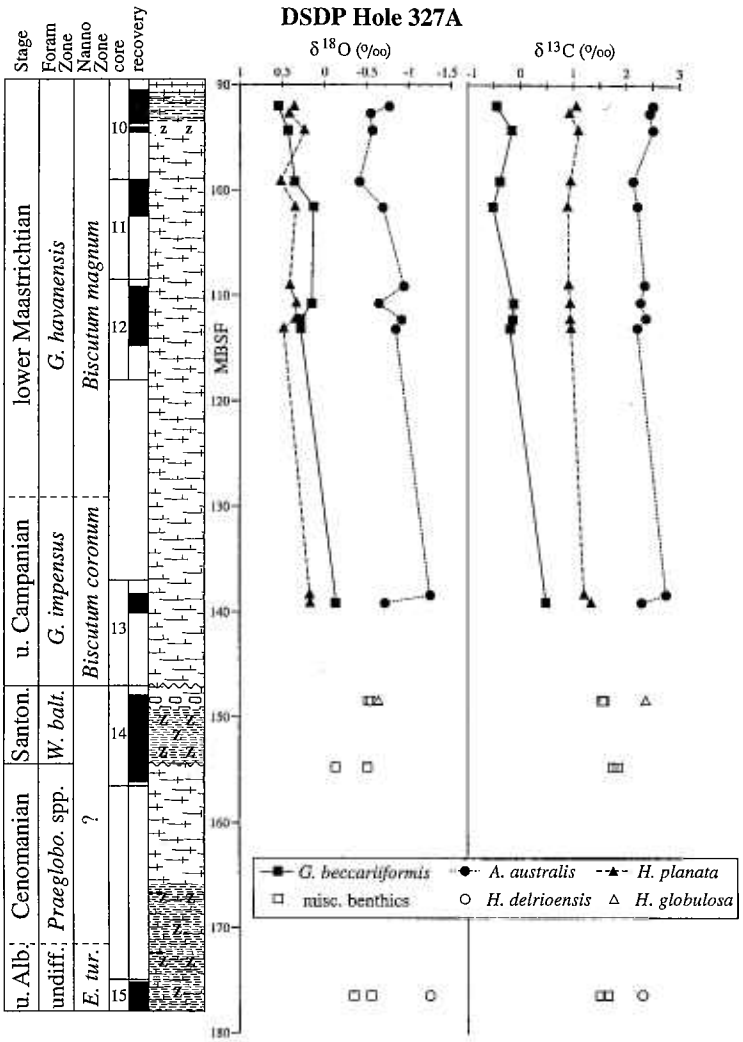

Figure 5. Oxygen and carbon isotopic plots for 40 samples of benthic and planktonic foraminifera from Deep Sea Drilling Project Hole 327A shown relative to the Cretaceous stages, planktonic foraminiferal and calcareous nannoplankton biostratigraphy, core recovery, and lithology. Isotopic data are presented in Table 3.

Campanian. Minor recrystallization can be detected in the upper Cenomanian and upper Albian planktonic foraminifera shown in Figure 7b. The inner chamber walls and the pore cross-sections are not as smooth as in Figure 7a, and the calcite of both specimens has a blockier appearance. Nonetheless, shell microlayering is still clearly discernible, indicating that, if precipitation of secondary calcite has occurred, it must be volumetrically very minor. Foraminifera from the lower Maastrichtian of Hole 327A exhibit excellent preservation with no shell recrystallization, particularly in clay-rich intervals (Fig. 7c). Shell recrystallization is apparent in late Albian foraminifera from Hole 327A, but absence of calcite rhombs on the inner chamber wall indicates that there has been minimal introduction of secondary calcite (Fig. 7d). Recrystallization is more severe in the Turonian–Santonian chalk samples from Site 258; shell recrystallization has obscured shell microlayering, and secondary calcite overgrowth is apparent on the inner chamber walls of foraminifera from core 258-5 (Fig. 8a). Sample 258-14-1, 121 cm, yields well-preserved foraminifera, however, with no evidence of secondary calcite overgrowth or shell recrystallization (Fig. 8b). Abundant clay at this level may have impeded exchange of pore waters enriched with dissolved calcium carbonate. The worst preservation among the samples we analyzed occurs in Albian and early Campanian foraminifera from tropical Site 305. Scanning electron microscope views of planktonic foraminifer chamber interiors from this site reveal calcareous nannofossils that are cemented to the shell wall and large crystals of euhedral calcite, as well as complete obliteration of the shell microstructure, but pores in the shell wall are still open (Figs. 8c and 8d).

In addition to preservation that is visually good to excellent, isotopic differences between taxa argues against significant diagenetic alteration. Replacement or reprecipitation of secondary calcite can homogenize the isotopic signals of different species or selectively modify ratios in different taxa. Hence, single taxon plots from samples with little or no diagenetic alteration show relatively constant interspecies differences, whereas similar plots from strongly altered material tend to cross or converge.

ISOTOPIC RESULTS

DSDP Site 511, Falkland Plateau

Oxygen Isotopes. Oxygen isotope records were obtained for 14 species of planktonic foraminifera from the Albian–lower Maastrichtian of Site 511 (Table 2 and Fig. 3). The Albian planktonic

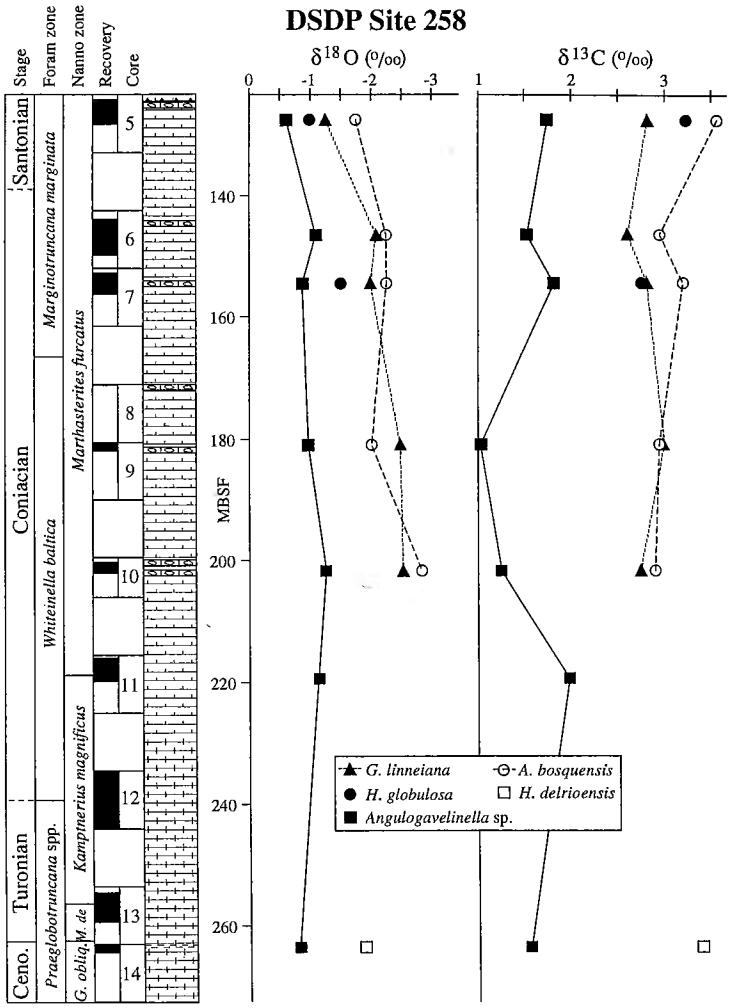

Figure 6. Oxygen and carbon isotopic plots for 20 samples of benthic and planktonic foraminifera from Deep Sea Drilling Project Site 258 shown relative to the Cretaceous stages, planktonic foraminiferal and calcareous nannoplankton biostratigraphy, core recovery, and lithology. Isotopic data are presented in Table 4.

record shows relatively little change, with values averaging about −1.0‰ and ranging from −0.7‰ to −1.2‰. Planktonic $\delta^{18}O$ values decrease to −2.3‰ in the upper Cenomanian and further decrease to −4.4‰ at the base of the Turonian interval, which is the most negative of the Site 511 sequence. Planktonic species exhibit a range of $\delta^{18}O$ values in the Coniacian–Santonian interval, with the more negative species (*A. australis* and *A. bosquensis*) averaging about −3.2‰ and the more positive species (*H. globulosa* and *G. alvarezi*) averaging −1.6‰. Lower Campanian planktonic species also exhibit a broad range of $\delta^{18}O$ values, with the lowest values varying between −3.1‰ and −3.7‰ (alternately recorded by *A. australis*, *G. bulloides*, *Hedbergella* sp. 4, and *H. globulosa*), and the highest values approaching −1.0‰ (alternately recorded by *G. alvarez*, *A. cretacea*, and *H. globulosa*). A shift to higher (i.e., cooler) planktonic $\delta^{18}O$ values begins in the upper part of the lower Campanian and progressively decreases to −0.7‰ in the lower Maastrichtian.

Benthic $\delta^{18}O$ values from Site 511 were obtained from 16 different species but are represented by one symbol in Figure 3. The resulting curve roughly parallels the trend of minimum $\delta^{18}O$ values recorded by planktonic foraminifera. Benthic $\delta^{18}O$ values gradually decrease from a maximum of 0.5‰ in the lower Albian to −0.4‰ in the upper Cenomanian, then further decrease to −1.5‰ in the Turonian. Turonian–lower Campanian benthic $\delta^{18}O$ values remain relatively low, varying between about −0.9‰ to −1.5‰, until cores 511-31 through -28, where the benthic $\delta^{18}O$ values average −0.7‰. Benthic oxygen isotopes further increase in the upper Campanian, with values averaging −0.1‰, to a lower Maastrichtian maximum of 0.4‰.

Carbon Isotopes. Planktonic foraminifer carbon isotope ratios exhibit little change in the Albian, with values averaging 2.4‰ (Fig. 3). Mean planktonic $\delta^{13}C$ values decrease to a minimum of 0.6‰ in the upper Cenomanian, then increase to 1.6‰ in the Turonian, and further increase to 2.3‰ in the Coniacian–Santonian. The heaviest $\delta^{13}C$ compositions are recorded in the lower Campanian by *H. globulosa*, *Hedbergella* sp. 4, *A. australis*, and *G. bulloides*, which mostly range between 3.0‰ and 3.7‰ in cores 511-39 through -30. Planktonic $\delta^{13}C$ values progressively decrease in the upper part of the lower Campanian to an average of 1.4‰ in core 511-28, then increase to an average of 2.3‰ in the upper Campanian and again decrease to an average of 1.5‰ in the lower Maastrichtian.

There are a number of sharp changes in the benthic carbon isotope curve from Site 511, but most of these occur as single inflection points and may be artifacts of fractionation differences between the species analyzed in the adjacent samples. The highest

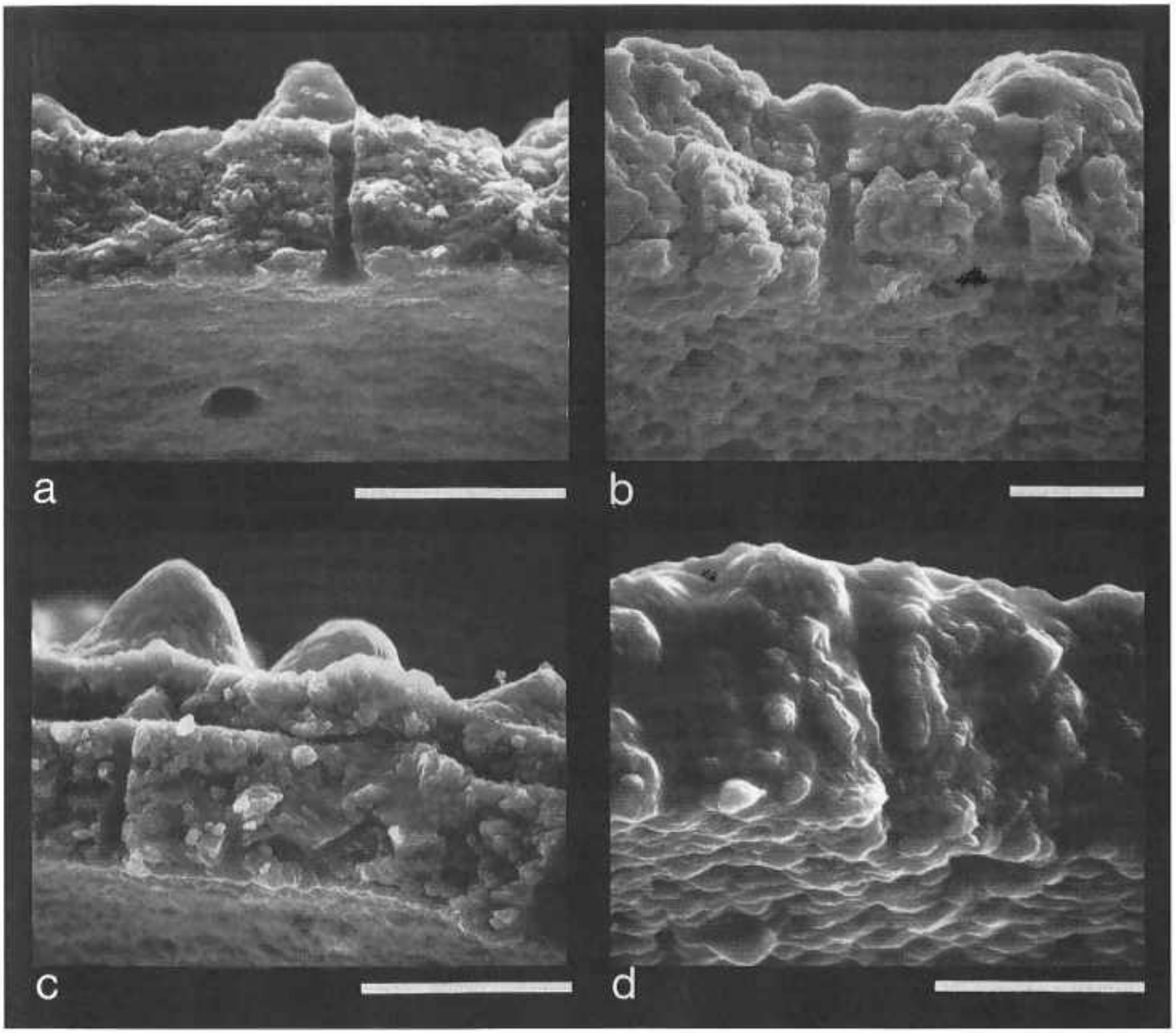

Figure 7. Cross-sectional view of penultimate chamber interior in foraminifera from Deep Sea Drilling Project Sites 327 and 511. Scale bar represents 5 μm. (a) Lower Campanian *Hedbergella* sp. 4 from sample 511-32-5, 20–24 cm; note absence of secondary calcite and no evidence of shell recrystallization. (b) Upper Cenomanian *Whiteinella baltica* from sample 511-48-1, 24–27 cm; note minor recrystallization of shell wall, but absence of secondary calcite. (c) Lower Maastrichtian *Archaeoglobigerina australis* from sample 327A-10-2, 136–138 cm; note absence of secondary calcite and no evidence of shell recrystallization. (d) Upper Albian *Hedbergella delrioensis* from sample 327A-15-2, 13–15 cm; note that the shell is recrystallized, but there is no evidence for secondary calcite.

benthic $\delta^{13}C$ values in the Cretaceous sequence average 2.2‰ in the lower Albian. Benthic $\delta^{13}C$ values average 1.1‰ in the middle and upper Albian, decrease to 0.2‰ in the uppermost Cenomanian, further decrease to an average of 0.0‰ in the Turonian, and average −0.3‰ in the lower part of the Coniacian–Santonian (core 511-46). Higher in the Coniacian–Santonian, benthic $\delta^{13}C$ values average 1.0‰. Lower Campanian benthic $\delta^{13}C$ values are quite variable, first decreasing to 0.0‰, next increasing to ≈1.0‰, and then widely fluctuating between −0.5‰ and 1.5‰. Benthic $\delta^{13}C$ values vary between ≈0.6‰ and 1.3‰, and average 0.9‰ in the upper Campanian, then decrease to 0.0‰ in the lower Maastrichtian.

DSDP Hole 327A, Falkland Plateau

Oxygen Isotopes. The Cretaceous foraminiferal oxygen isotope record from Site 327 is far less complete than from Site 511 because of extensive coring gaps, poor core recovery, disconformities, and

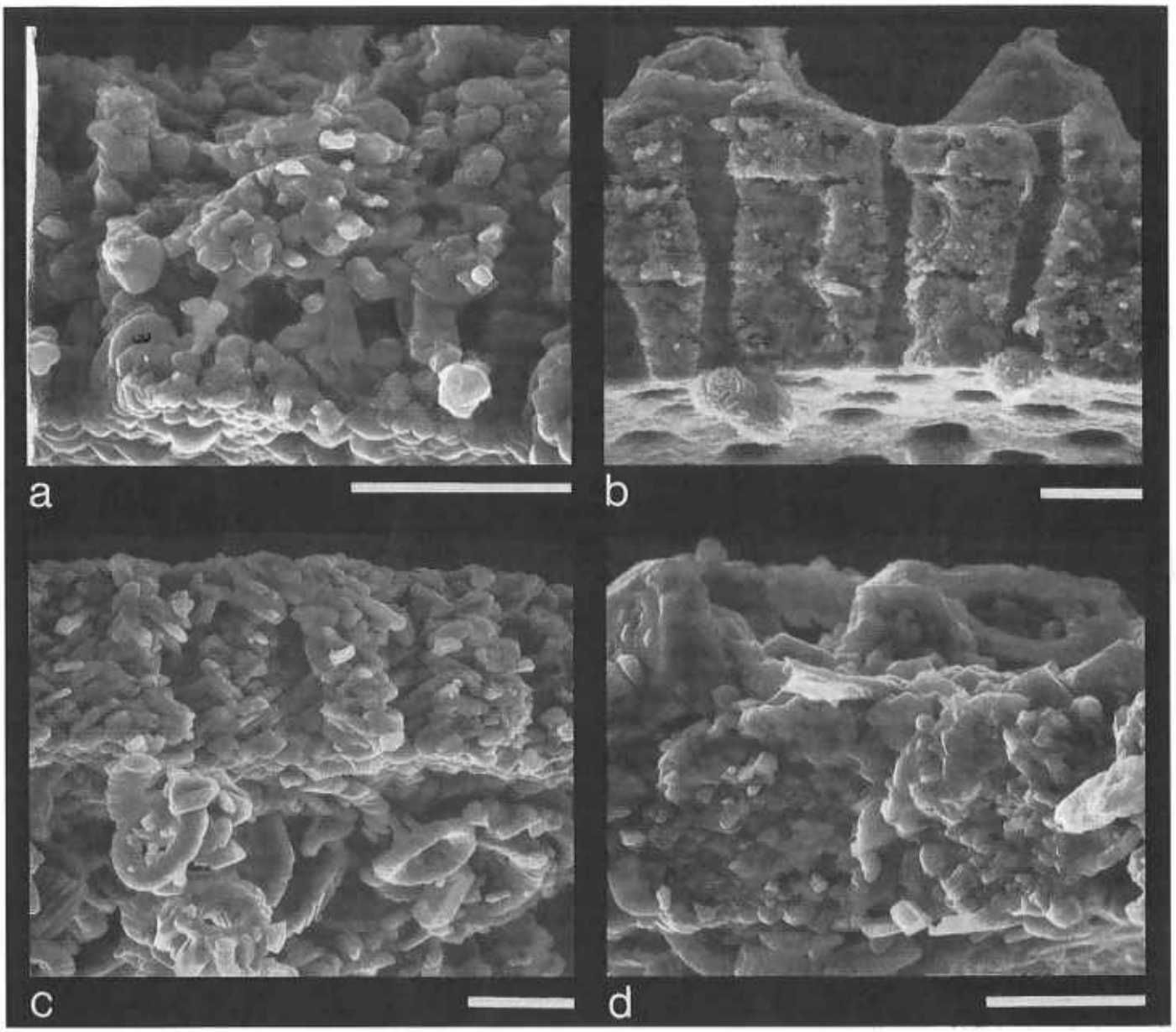

Figure 8. Cross-sectional view of penultimate chamber interior in foraminifera from Deep Sea Drilling Project Sites 258 and 305. Scale bar represents 5 μm. (a) Santonian *Archaeoglobigerina bosquensis* from sample 258-5-3, 108–111 cm; note minor presence of secondary calcite and significant shell recrystallization. (b) Cenomanian *Hedbergella delrioensis* from sample 258-14-1, 83–86 cm; note that there is no evidence of shell recrystallization or presence of secondary calcite. (c) lower Campanian *Globotruncanita stuartiformis* from sample 305-25-2, 80–84; note substantial shell recrystallization and significant presence of secondary calcite cementing calcareous nannoplankton and in the form of euhedral rhombs. (d) upper Albian *Hedbergella delrioensis* from sample 305-41-CC; note significant shell recrystallization, but minor presence of secondary calcite.

severe dissolution in several cores. Results are presented for only five sample levels for the upper Albian–upper Campanian interval, but a more continuous record was obtained from the lower Maastrichtian interval (Fig. 5 and Table 3).

The planktonic foraminifer *H. delrioensis* yielded a $\delta^{18}O$ value of −1.3‰ for the upper Albian, which is ≈0.8‰ lighter than values obtained from co-occurring benthic foraminifera. Santonian $\delta^{18}O$ measurements from benthic foraminifera are about the same as in the upper Albian, averaging −0.4‰. The planktonic $\delta^{18}O$ value recorded by the biserial *H. globulosa* in the Santonian is only 0.1‰ lighter than the values from co-occurring benthic foraminifera. Benthic foraminifer $\delta^{18}O$ values recorded by *G. beccariiformis* become progressively heavier by ≈0.7‰ from the upper Campanian through the lower Maastrichtian. $\delta^{18}O$ values of the planktonic *A. australis* also increase through this interval, with upper Campanian values averaging −1.0‰ and lower Maastrichtian values averaging −0.7‰. Similar to *H. globulosa* in the Santonian, the $\delta^{18}O$ measurements obtained from the biserial planktonic *H. planata* plot very

close to the co-occurring benthic values throughout the upper Campanian–lower Maastrichtian interval.

Carbon Isotopes. The carbon isotope data from Site 327 reveal consistent differences between the foraminifer species analyzed, with all planktonic taxa plotting heavier than the benthic taxa (Fig. 5 and Table 3). Benthic $\delta^{13}C$ values are very similar in the upper Albian and Santonian, averaging 1.6‰. The benthic $\delta^{13}C$ values recorded by *G. beccariiformis* show a progressive decrease from 0.5‰ in the upper Campanian to −0.5‰ in the lower Maastrichtian. Planktonic $\delta^{13}C$ values from *H. delrioensis* in the upper Albian and *H. globulosa* in the Santonian are 2.3‰ and 2.4‰, respectively. The $\delta^{13}C$ values recorded by *A. australis* are nearly the same in the upper Campanian and lower Maastrichtian, averaging 2.5‰. Likewise, $\delta^{13}C$ measurements from *H. globulosa* show little change throughout the upper Campanian–lower Maastrichtian interval, averaging 1.0‰.

DSDP Site 258, Naturaliste Plateau

Oxygen Isotopes. Benthic $\delta^{18}O$ measurements obtained from *Angulogavelinella* sp. at Site 258 decrease from −0.8‰ in the Cenomanian to an average of −1.0‰ in the Coniacian–Santonian of cores 258-6 through -11 (Fig. 6 and Table 4). In core 258-5, the oxygen isotopic composition of *Angulogavelinella* sp. increases to −0.6‰. Planktonic $\delta^{18}O$ values also decrease from the Cenomanian into the Coniacian–Santonian, with *H. delrioensis* yielding −1.9‰ in the Cenomanian and *A. bosquensis* and *G. linneiana* averaging −2.3‰ in cores 258-6 through -11. The average $\delta^{18}O$ value for the last two species increases to −1.5‰ in core 258-5. *Heterohelix globulosa* yields the heaviest $\delta^{18}O$ values of the planktonic species analyzed, plotting closer to the benthic values, whereas *A. bosquensis* usually has the lightest planktonic $\delta^{18}O$ values. *Globotruncana linneiana* is usually ≈0.2‰ lower in $\delta^{18}O$ than *A. bosquensis.*

Carbon Isotopes. The benthic foraminifer *Angulogavelinella* sp. yields a Cenomanian $\delta^{13}C$ value of 1.6‰ and Coniacian–Santonian $\delta^{13}C$ values that vary from 1.0‰ to 1.8‰ (Fig. 6). The $\delta^{13}C$ measurements from planktonic foraminifera are consistently higher than from *Angulogavelinella*, with *Hedbergella delrioensis* yielding 3.4‰ in the Cenomanian and mean values of *A. bosquensis* and *G. linneiana* increasing from 2.9‰ to 3.2‰ in the Coniacian–Santonian. *Archaeoglobigerina bosquensis* has the highest $\delta^{13}C$ values in nearly all the Coniacian–Santonian samples, whereas *H. globulosa* and *G. linneiana* interchange as the planktonic species with the lowest $\delta^{13}C$ values.

DSDP Site 305, Western Equatorial Pacific

Two planktonic species from one upper Albian sample and two lower Campanian samples were analyzed for their stable isotopic composition (Table 5). Benthic foraminifera in these samples were too rare to be picked for isotopic study. The purpose of the analyses was to compare the results with the upper Albian and lower Campanian isotopic values that were published for Site 305 by Douglas and Savin (1973, 1975).

In both cases our values and those of Douglas and Savin (1973, 1975) are very similar. The upper Albian sample of *H. delrioensis* from core 305-41-CC yielded an oxygen isotopic composition of −3.3‰, which is only 0.1‰ lighter than the same species analyzed from core 305-42-CC by Douglas and Savin (1973), and the carbon isotopic compositions differed by 0.3‰. The $\delta^{18}O$ composition of *R. greenhornensis* run in this study, −2.7‰, is 0.3‰ lighter than *R. gandolfi* run by Douglas and Savin (1973, 1975), and the carbon isotopic compositions of these two sets of analyses differ by 0.1‰. Only bulk carbonate samples were run by Douglas and Savin (1973, 1975) for the lower Campanian, so no direct comparisons between planktonic taxa is possible. Nonetheless, the analyses of *G. stuartiformis* and *G. linneiana* from cores 305-25 and -26 yield oxygen isotopic compositions between −0.9‰ and −1.4‰, which is close to the −1.2‰ to −1.5‰ range reported for bulk carbonate from cores 305-25 through -27.

DISCUSSION

Planktonic Foraminiferal Depth Rankings

Temperature is one of the most important factors governing the vertical and geographic distribution of planktonic foraminifera (Bé, 1977; Hemleben et al., 1989). Since the $^{18}O/^{16}O$ ratio of calcite precipitated in equilibrium with the ambient water is temperature dependent, and temperature decreases with depth from the ocean surface, interspecies differences in $\delta^{18}O$ measured from modern planktonic foraminifera reflect growth at different levels in the water column (Emiliani, 1954; Shackleton and Vincent, 1978; Fairbanks and Weibe, 1980; Fairbanks et al., 1982). Species yielding higher $\delta^{18}O$ values are associated with deeper (cooler) surface-water habitats. Depth rankings of modern planktonic foraminifera based on oxygen isotopes have been confirmed by plankton tow and sediment trap studies (e.g., Berger, 1971; Bé, 1977; Deuser et al., 1981).

The fractionation of carbon isotopes in the upper water column is controlled by photosynthesis rather than temperature. Upper surface waters tend to be enriched in ^{13}C because the lighter carbon isotope (^{12}C) is preferentially removed from the ambient water by phytoplankton. As the phytoplankton die and sink through the water column, the ^{12}C-enriched organic matter is oxidized and released. Thus, the shells of planktonic foraminifera that calcified in the upper surface waters are relatively enriched in $\delta^{13}C$, whereas those calcified at deeper levels are more depleted in $\delta^{13}C$ (Shackleton and Vincent, 1978; Spero and Williams, 1989).

Problems associated with using stable isotopes to infer depth habitats among planktonic foraminifera have been reviewed by several authors (Wefer and Berger, 1991; Corfield and Cartlidge, 1991; D'Hondt and Arthur, 1995). In addition to depth, interspecies differences in $\delta^{18}O$ and $\delta^{13}C$ may be influenced by (1) the kinetic effects of different calcification rates for different species and changes in calcification rates during ontogeny, (2) shell growth during different seasons, (3) the presence of algal symbionts, (4) measurement error (generally ±0.1‰), and (5) differential preservation. To minimize ontogenetic and preservation effects, only the largest, best preserved specimens of the most abundant species were chosen for isotopic analysis. But the influence of vital and seasonal effects on Cretaceous species have not been determined.

Depth habitats inferred for Cretaceous planktonic foraminifera have been based on morphological analogies with depth-stratified living planktonic foraminifera (Hart, 1980; Caron and Homewood, 1983), biofacies profile comparisons in continental margin settings (Sliter, 1972; Hart and Bailey, 1979; Leckie, 1987), and limited stable isotope data (e.g., Douglas and Savin, 1978; Boersma and Shackleton, 1981; Corfield et al., 1990). These studies generally concluded that keeled (e.g., globotruncanid) and other heavily calcified taxa

lived at deeper levels in the surface waters than thinner-walled, nonkeeled (e.g., heterohelicid, hedbergellid) taxa. Planispiral Cretaceous taxa (e.g., *Globigerinelloides*) have been considered as both shallow and deep dwellers by different authors (e.g., Boersma and Shackleton, 1981; Barrera and Hubcr, 1990). More recently, D'Hondt and Arthur (1995) demonstrated a greater complexity in morphotypic depth distributions than earlier models suggcsted. Their isotopic analyses of late Maastrichtian planktonic foraminifera indicate that heterohelicids and globotruncanids spanned a wide range of surface-water habitats, with some heterohelicid species yielding the highest (coolest) $\delta^{18}O$ signals and some globutruncanid species yielding the lowest (warmest) $\delta^{18}O$ signals. Results obtained in this study also demonstrate exceptions to the morphotypic-based models used to infer Cretaceous planktonic foraminiferal depth habitats.

The simplest way to characterize isotopic diffcrences among foraminifcra that may be related to depth is to plot $\delta^{18}O$ versus $\delta^{13}C$ values from different species at several time intervals. This is depicted in Figure 9 for planktonic and benthic foraminifera from core intervals in the Turonian–Coniacian, lower Campanian, and upper Campanian–lower Maastrichtian at Site 511, the lower Maastrichtian at Site 327, and the Coniacian–Santonian at Site 258. Assuming that all species fractionated at or near isotopic equilibrium and seasonal effects were minimal, planktonic species with the most negative $\delta^{18}O$ values and most positive $\delta^{13}C$ values within each time interval are considered as the shallowest dwelling taxa. Our results show that *A. australis*, *A. bosquensis*, and *Hedbergella* spp. consistently plot farthest from the benthic foraminifcr values, suggesting that they lived in an upper surface-water paleohabitat. The isotopic values exhibited by the keeled species *G. bulloides* and *G. linneiana* are close to those of *A. australis* and *A. bosquensis* and also indicate a near-surface-water paleohabitat. On the other hand, the isotopic values of *A. cretacea*, *M. marginata*, *P. stephani*, and *G. alvarezi* plot closest to the benthic isotopic values, indicating growth at deeper levels in the surface waters. *Whiteinella baltica* yields isotopic values bctween those of the deepest and shallowest planktonic species.

Depth ranking estimates for the biserial taxon *Heterohelix* may differ strongly from one stratigraphic interval to another and even within the same sample. For example, within sample 511-36-6, 23-27, one analysis of *H. globulosa* yields 2.7‰ lower $\delta^{18}O$ and 2.2‰ higher $\delta^{13}C$ values than an analysis of *Heterohelix* spp. from the same sample (Table 2). Samples of *H. globulosa* and *Heterohelix* spp. in the interval from core 511-38 to -40 yield $\delta^{18}O$ and $\delta^{13}C$ values that are close to benthic isotopic values. This inconsistency is repeated at other intervals in the lower Campanian, including core 511-34 to -37, where *H. globulosa* plots as a near-surface taxon and *Heterohelix* spp. plots deeper than any of the other species measured, and core 511-30 to -33, where *Heterohelix* spp. gives both shallow and deep isotopic compositions (Fig. 9). Isotopic analyses of heterohelicids from the upper Campanian and lower Maastrichtian intervals at Sites 327 and 511 consistently yield $\delta^{18}O$ and $\delta^{13}C$ values that are close to or overlap with those from co-occurring benthic species. Because it is unlikely that these isotopic compositions reflect a benthic habitat, given the much greater abundance of heterohelicids relative to any benthic species from these sites, they may result from an unusually strong vital effect or growth below the thermocline within an oxygen minimum zone. Boersma and Premoli Silva (1989) have inferred such an oxygen minimum habitat for biserial taxa during the Paleocene.

Composite Isotopic Curve for the Southern High Latitudes

Stable isotope data reported in this study are combined with the Maastrichtian stable isotope record of Barrera and Huber (1990) for ODP Site 690 (lat 65°S) to reconstruct the history of oxygen and carbon isotopic change in the southern high latitudes from the Albian through Maastrichtian (Fig. 10). All benthic species are represented by one symbol and planktonic species are combined into biserial, planispiral, low and high trochospiral, and keeled planktonic morphogroups, which are represented as separate symbols (see caption of Fig. 10 for species groupings). The plots for the Albian–lower Campanian interval are based primarily on isotopic data from Site 511, but include Cenomanian and Coniacian–Santonian data from Site 258. The plots for the upper Campanian–Maastrichtian interval are based on isotopic data from Sites 511, 327, and 690, which are correlated using foraminiferal and nannofossil biostratigraphy and strontium isotopic ratios, as was discussed previously.

Isotopic palcotemperatures were calculated using the equation

$$T\,°C = 16.998 - 4.52(\delta_c - \delta_w) + 0.28(\delta_c - \delta_w)^2 \qquad (1)$$

(Erez and Lutz, 1983), where $\delta_c = \delta^{18}O$ of CO_2 generated by reaction of the carbonate with phosphoric acid relative to Pee Dee belemnite, and $\delta_w = -1‰$, which is the $\delta^{18}O$ (standard mean ocean water) for ice-free conditions in polar regions during the middle–Late Cretaceous (Shackleton and Kennett, 1975). When minimum $\delta^{18}O$ values from each sample level are substituted into the paleotemperature equation, temperatures inferred for the upper surface watcrs are estimated as ≈17 °C in the Albian, increasing to ≈23 °C in the Cenomanian, reaching ≈33 °C in the Turonian, and ranging between ≈27 and 31 °C from the Turonian through most of the lower Campanian. A unidirectional cooling trend begins in the lower Campanian and continues through the Maastrichtian with the coolest near-surface-water temperatures estimated as 10 °C in the uppermost Maastrichtian. The Turonian–lower Campanian temperatures seem excessively warm for a paleolatitude of 56°S–60°S cven during the Cretaceous ultrathermal. Potential sources of error include diagcnetic alteration or an incorrect value for the $\delta^{18}O_w$ of water in the temperature equation.

Ironically, of all the planktonic foraminifera examined in this study, those that yield the least plausible paleotemperature estimates show the best preservation. Some workers have argued that even the best preserved foraminiferal tests undergo some recrystrallization during diagenesis, and it is impossible to tell visually whether a foraminifer has been altered or not (Richter and DePaolo, 1988; Schrag et al., 1992). The close association between the interval of depleted $\delta^{18}O$ values and the occurrence of zeolitic clays in Site 511 is suspicious. The zeolites (heulandite) in Site 511 have been interpreted as being derived from fine, basaltic, volcaniclastic material (Varentsov et al., 1983). Oxygen isotope studies of pore waters have shown large $\delta^{18}O$ depletions that are associated with alteration of volcanic material at this site, especially in carbonate-poor sediments such as those found at Site 511 (Lawrence et al., 1979; Gieskes, 1981; Gieskes and Lawrence, 1981; Pisciotto, 1981). Carbonatcs that have undergonc even minor recrystallization in such depleted pore waters might show significant depletions in $\delta^{18}O$ values, similar to those observed for Site 511.

Although diagenesis seems like the most plausible explanation for the highly depleted $\delta^{18}O$ values mcasured in Site 511, several points argue against this intcrpretation. First, the scanning clectron

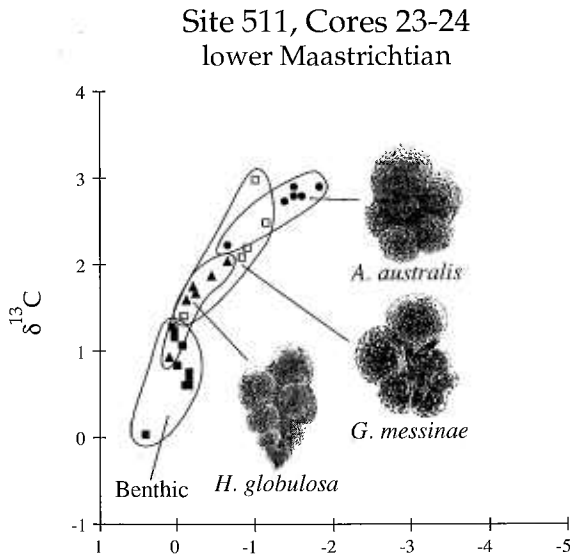
Site 511, Cores 23-24
lower Maastrichtian
δ13C
A. australis
G. messinae
H. globulosa
Benthic

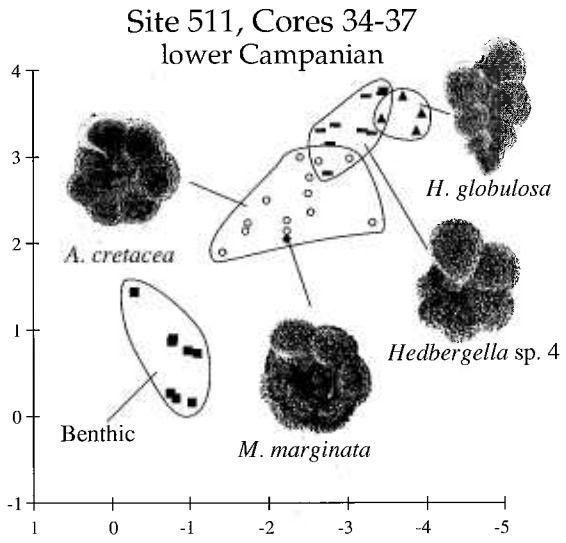
Site 511, Cores 34-37
lower Campanian
H. globulosa
A. cretacea
Hedbergella sp. 4
Benthic
M. marginata

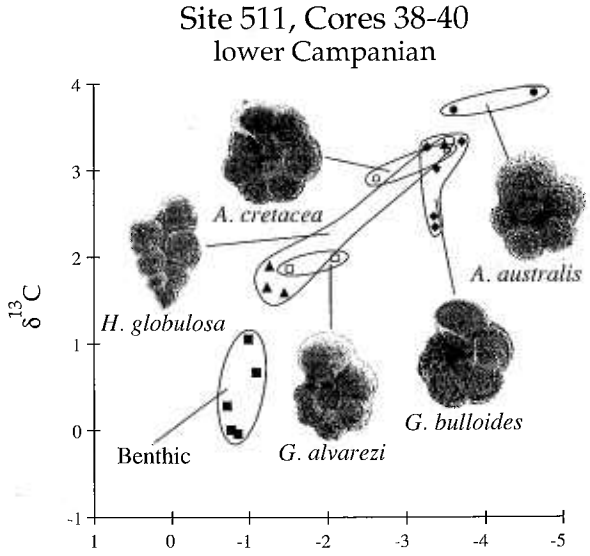
Site 511, Cores 38-40
lower Campanian
δ13C
A. cretacea
A. australis
H. globulosa
G. bulloides
Benthic
G. alvarezi

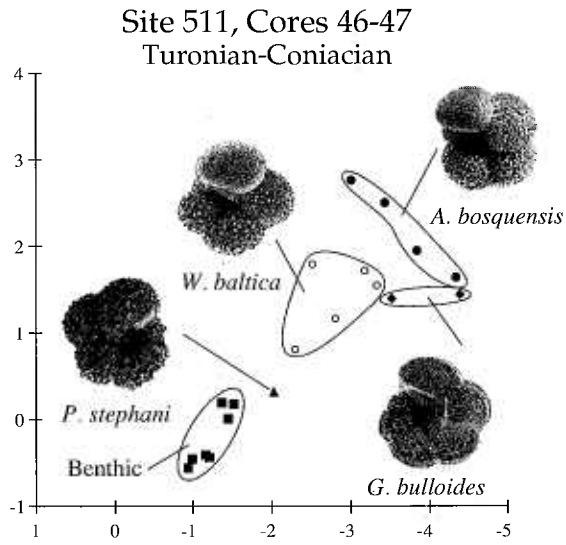
Site 511, Cores 46-47
Turonian-Coniacian
A. bosquensis
W. baltica
P. stephani
Benthic
G. bulloides

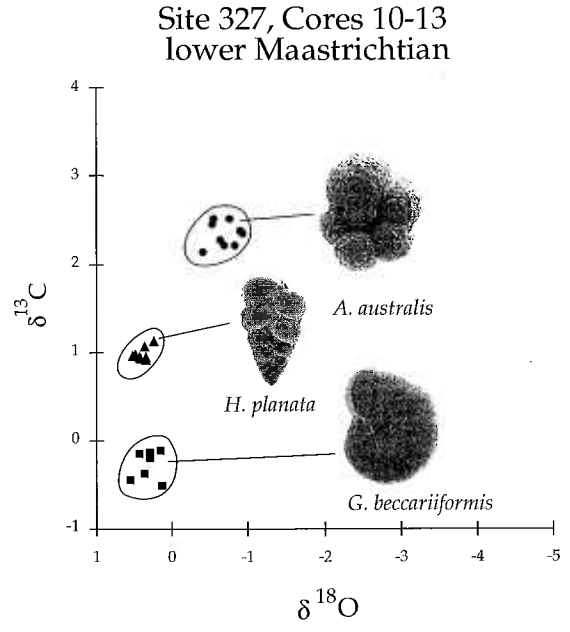
Site 327, Cores 10-13
lower Maastrichtian
δ13C
A. australis
H. planata
G. beccariiformis
δ18O

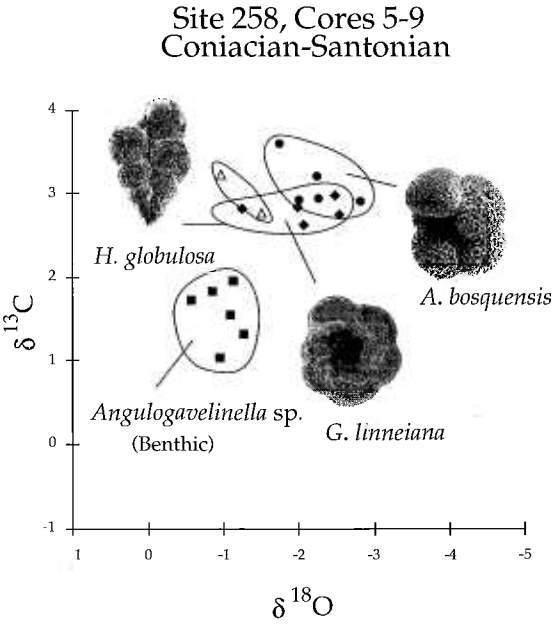
Site 258, Cores 5-9
Coniacian-Santonian
δ13C
H. globulosa
A. bosquensis
Angulogavelinella sp.
(Benthic)
G. linneiana
δ18O

Figure 9. Plots of $\delta^{18}O$ vs. $\delta^{13}C$ data for planktonic and benthic foraminifera from core intervals in the Turonian–Coniacian, lower Campanian, and upper Campanian–lower Maastrichtian at Site 511, the lower Maastrichtian at Site 327, and the Coniacian–Santonian at Site 258. Planktonic samples with light $\delta^{18}O$ and heavy $\delta^{13}C$ compositions are inferred to have lived in shallower surface waters than those with heavy $\delta^{18}O$ and light $\delta^{13}C$ values.

photomicrographs of planktonic foraminifera from Site 511 indicate extraordinarily good preservation (Figs. 7a and 7b). Second, the $\delta^{18}O$ and $\delta^{13}C$ values of multiple planktonic foraminiferal species from Site 511 give a consistent, reasonable pattern of depth distribution for each species (Fig. 9). The diagenesis would have had to have shifted the absolute $\delta^{18}O$ values, but maintained the relative $\delta^{18}O$ differences between species. Finally, strontium isotopic measurements of Site 511 foraminifera are consistent with expected $^{87}Sr/^{86}Sr$ values of seawater for the time period (Fig. 4). If strontium isotopic exchange had occurred between foraminifera and interstitial waters during diagenesis, we would expect markedly different $^{87}Sr/^{86}Sr$ values (Lawrence et al., 1979).

Alternatively, the $\delta^{18}O_w$ value of $-1‰$ standard mean ocean water we assumed for calculating paleotemperatures may be inappropriate for Cretaceous seawater at Site 511. To bring the paleotemperatures in line with other studies, the $\delta^{18}O_w$ of surface and deep waters at Site 511 would have to be significantly less than the mean isotopic composition of $-1‰$ used for the Cretaceous ocean. For example, reduced salinity of waters at Site 511 during the Turonian–late early Campanian might account for the low $\delta^{18}O$ values measured in foraminiferal calcite. Tectonic uplift to the south along the North Scotia Ridge, or to the west in the southern Andes, may have led to climatic changes including increased runoff and an influx of lower-salinity waters. In this scenario, planktonic foraminifera would have recorded lower $\delta^{18}O$ values, but it is unlikely that the $\delta^{18}O$ of benthic foraminifera would have been significantly affected. At Site 511, the benthic and planktonic $\delta^{18}O$ records show parallel trends, suggesting that the environmental changes affected the entire water column rather than just the surface mixed layer.

Vertical Isotopic Gradients

Insight into variations in the thermal stratification of the water column and surface-water productivity can be gained by comparison of surface- to bottom-water gradients in $\delta^{18}O$ and $\delta^{13}C$. These isotopic gradients are determined from the maximum differences in planktonic and benthic $\delta^{18}O$ and $\delta^{13}C$ values (denoted as $\Delta\delta^{18}O$ and $\Delta\delta^{13}C$) for all samples analyzed. Generally, the larger the $\delta^{18}O$ gradient, the greater the vertical thermal stratification, and the larger the $\delta^{13}C$ gradient, the higher the surface productivity.

At Site 511, the $\Delta\delta^{18}O$ ranged between $\approx$1.0‰ and 1.2‰ ($\approx$4–6 °C) during the Albian, it increased to $\approx$1.7‰ ($\approx$7 °C) during the upper Cenomanian, and the $\delta^{18}O$ gradient increased dramatically to nearly 3‰ ($\approx$12 °C) during the Turonian. There are few samples with planktonic and benthic isotopic data from the Coniacian–Santonian at Site 511, but the available results indicate $\Delta\delta^{18}O$ values of $\approx$1.7‰, except in core 511-43 where there is a 2.6‰ oxygen isotopic gradient. The vertical $\delta^{18}O$ gradient is quite high for most of the lower Campanian, fluctuating between $\approx$2.3‰ and 3.0‰. This diminishes to $\approx$1.5‰ in the upper Campanian, then to $\approx$1.0‰ in the lower Maastrichtian.

The $\delta^{18}O$ gradients recorded at Site 327 are similar to those from Site 511 for the Albian and the lower Maastrichtian, but the upper Campanian vertical gradient recorded in core 327-13 is lower by $\approx$0.4‰. Vertical $\delta^{18}O$ gradients at Site 258 are also lower than at correlative levels at Site 511, averaging $\approx$1.0‰ in the Cenomanian and ranging from 1.2‰ to 1.6‰ in the Coniacian–Santonian. Results from Site 690 (Barrera and Huber, 1990) indicate that $\Delta\delta^{18}O$ reached minimum values of $\approx$0.5‰ ($\approx$2 °C) in the late Maastrichtian.

The carbon isotopic gradient at Site 511 shows little change in the Albian, with $\Delta\delta^{13}C$ values fluctuating between 0.9‰ and 1.4‰. Cenomanian $\Delta\delta^{13}C$ values range from 0.6‰ to 1.2‰. Turonian $\Delta\delta^{13}C$ values are higher, at $\approx$1.8‰, then Coniacian–Santonian values reach as high as 2.6‰. Surface- to deep-water $\Delta\delta^{13}C$ is quite high in the lower Campanian, reaching values >2.3‰ in most samples and >3.5‰ in several samples. The $\delta^{13}C$ gradient decreases to 1.4‰ in core 511-28, then fluctuates between 2.1‰ and 2.2‰ through the upper Campanian and lower Maastrichtian.

$\Delta\delta^{13}C$ values from Site 327 are similar to those obtained from Site 511. They are $\approx$0.8‰ in the Albian and Cenomanian, reach 1.8‰ in the upper Campanian, and range from 2.3‰ to 2.7‰ in the lower Maastrichtian. At Site 258, $\Delta\delta^{13}C$ values from the Cenomanian approximate Cenomanian values from Site 511, but $\Delta\delta^{13}C$ values in the Coniacian–Santonian interval are from 1.0‰ to 2.5‰ lower. The upper Maastrichtian $\Delta\delta^{13}C$ at Site 690 averages $\approx$1‰ (Barrera and Huber, 1990).

The general pattern of changes in $\Delta\delta^{13}C$ at Sites 511, 327, 258, and 690 are similar to the $\Delta\delta^{18}O$ record (Fig. 10). Gradients are low throughout the Albian, relatively moderate in most of the upper Cenomanian through Coniacian–Santonian, high throughout most of the lower Campanian, low in the upper part of the lower Campanian, then moderate in the upper Campanian and lower Maastrichtian and low in the upper Maastrichtian. These results suggest that the water column at southern high latitudes changed from being strongly mixed during the Albian, to moderately to well-stratified during the late Cenomanian through Coniacian–Santonian, to well-stratified during much of the early Campanian, to moderately mixed in the late Campanian and early Maastrichtian, and to strongly mixed in the late Maastrichtian.

Plots of simple planktonic species diversity and keeled planktonic species abundance through the Site 511 (Fig. 3) and Site 690 sequences (Huber, 1990) do not entirely support this interpretation if assumptions for Cretaceous planktonic foraminifer paleoecology are correct. Times of low species diversity with few, if any, keeled species are generally interpreted as periods when surface waters were well mixed and/or relatively cool, whereas times of high species diversity and high-keeled species abundance reflect periods when the water column was well stratified and surface waters were relatively warm (Douglas, 1969; Hart and Bailey, 1979; Caron and Homewood, 1983; Leckie, 1987). The species diversity plot in Figure 3 shows that total diversity is relatively constant and low throughout the Cenomanian–lower Maastrichtian sequence at Site 511, with 6 to 10 species in many samples. Levels where 12 or more species occur do not necessarily correspond with high $\delta^{18}O$ and $\delta^{13}C$ gradients or anomalously warm surface-water temperatures. For example, assemblages from 234.92 mbsf have a relatively high diversity

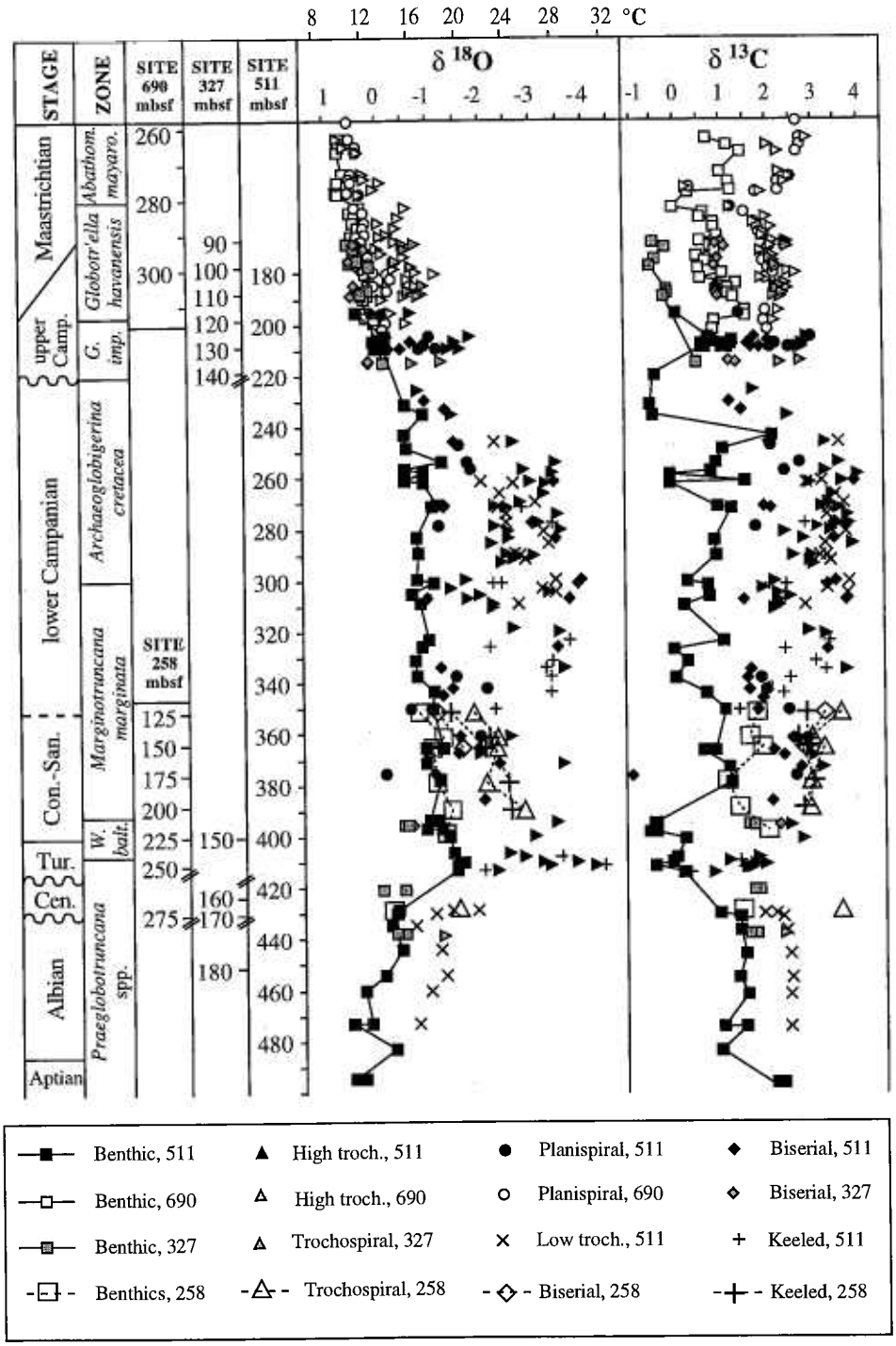

Figure 10. Composite oxygen and carbon isotopic curves for the southern high latitudes for Albian–late Maastrichtian time combining data from Ocean Drilling Program hole 690C (Maud Rise) and Deep Sea Drilling Project Sites 327 and 511 (Falkland Plateau), and DSDP Site 258 (Naturaliste Plateau). Scales for meters below sea floor are shown for each site, alongside the planktonic foraminiferal biozonation of Huber (1992). Morphologic groupings include the following genera: biserial (*Heterohelix*), planispiral (*Globigerinelloides*), low trochospiral (*Hedbergella*), high trochospiral (*Archaeoglobigerina* and *Whiteinella*), and keeled (*Globotruncana*, *Marginotruncana*, and *Praeglobotruncana*). All $\delta^{18}O$ values are expressed relative to the Pee Dee belemnite standard. Paleotemperature estimates were derived using the paleotemperature equation of Erez and Lutz (1983) assuming that the isotopic composition of the Maastrichtian was −1 per mil relative to standard mean ocean water.

(12 species), but oxygen isotopic results indicate a low vertical thermal gradient (≈2 °C) and a surface-water temperature that is ≈8 °C cooler than assemblages from 253.62 mbsf, which have only 9 species but indicate a vertical temperature gradient of ≈9 °C. Samples with six or fewer species generally correspond with dissolution intervals, as evidenced by a corresponding high abundance of benthic species and very low percent carbonate. Levels where keeled planktonics comprise >10% of the total planktonic assemblage do occur at times when there are high vertical $\delta^{18}O$ gradients, but keeled species also may be completely absent during these times.

A similar lack of correspondence between planktonic species diversity and oxygen isotopic paleotemperature trends was observed from the lower and upper Maastrichtian of Site 690; a poleward incursion of keeled planktonic species occurred at a time when surface waters cooled and vertical thermal gradients diminished (Huber, 1990; Barrera and Huber, 1990). Evidently, in addition to temperature and vertical mixing, hydrographic factors such as changes in the depth of the euphotic zone relative to the thermocline also influenced the planktonic species diversity and relative abundance trends at the high-latitude sites.

Surface-Water Latitudinal Isotopic Gradients

The oxygen isotope values of benthic and surface-dwelling planktonic foraminifera measured in this study and from the published literature have been plotted versus absolute paleolatitude for three time intervals (Fig. 11). Isotopic data for all three intervals are considered reliable, with the possible exception of Maastrichtian $\delta^{18}O$ values from Sites 305 and 463, which may have been diagenetically altered. The upper Maastrichtian interval was chosen because there are abundant isotopic data for this time period and because it represents the final phase of a long-term cooling trend that began during the late early Campanian. This interval comprises the foraminiferal *Abathomphalus mayaroensis* Total Range Zone at all sites. The Coniacian–Santonian interval represents one of the warmest phases of the Late Cretaceous climate. The late Albian interval is used because it precedes the Late Cretaceous ultrathermal.

The latitudinal $\delta^{18}O$ plots reveal several important points. Most significantly, all three Cretaceous reconstructions yield oxygen isotope values from surface mixed-layer planktonic foraminifera that are lower than in the Holocene (except for Sites 463 and 305 during the late Maastrichtian), but with the difference being greatest at high latitudes. Surface-water $\delta^{18}O$ from most tropical sites are lower than modern values by only ≈0.5‰ during the late Maastrichtian and Coniacian–Santonian, and by ≈1.5‰ in the late Albian. The difference between tropical and high-latitude planktonic foraminiferal $\delta^{18}O$ values amounts to ≈2.0‰ during the late Albian and ≈2.3‰ during the late Maastrichtian. Surprisingly, the Coniacian–Santonian latitudinal $\delta^{18}O$ gradient is reversed, with Site 511 surface water depleted in $\delta^{18}O$ by >1.00‰ relative to the tropical sites. Site 258 yields $\delta^{18}O$ values that are the same as or lower than the tropical sites. Such a distribution of surface-water $\delta^{18}O$ is unrealistic, suggesting that the $\delta^{18}O$ signatures may have been influenced by factors other than temperature.

The low-latitudinal $\delta^{18}O$ gradient for all three Cretaceous time intervals may be explained partly by differences in evaporation-precipitation balances, whereby tropical surface waters are relatively enriched in ^{18}O because of high net evaporation rates, and high-latitude surface waters are relatively depleted in ^{18}O because of high net precipitation rates. In the modern ocean, the $\delta^{18}O$ composition of surface waters is ≈1.5‰ higher in the tropics than at high latitudes because of Rayleigh fractionation during the net transport of water through the atmosphere from the warm surface ocean in low latitudes to the relatively cold surface ocean at high latitudes (Broecker, 1986). As a result of the $\delta^{18}O$ differences, tropical sea-surface temperatures calculated from Holocene $\delta^{18}O$ values of planktonic foraminifera underestimate the actual sea-surface temperatures by ≈3–4 °C (Zachos et al., 1994). Latitudinal differences in salinity probably have persisted throughout geologic time as the position of the Hadley cells, which control the areas of highest net evaporation, have remained fixed within the subtropics (Crowley and North, 1991). The pertinent question is whether the magnitude of the latitudinal salinity $\delta^{18}O$ gradient has remained constant through geologic time. Oceanic salinity gradients are controlled by the rate of water exchange between oceanic reservoirs, the rate of poleward water vapor transport (Broecker, 1986), and the extent of Rayleigh fractionation during vapor transport.

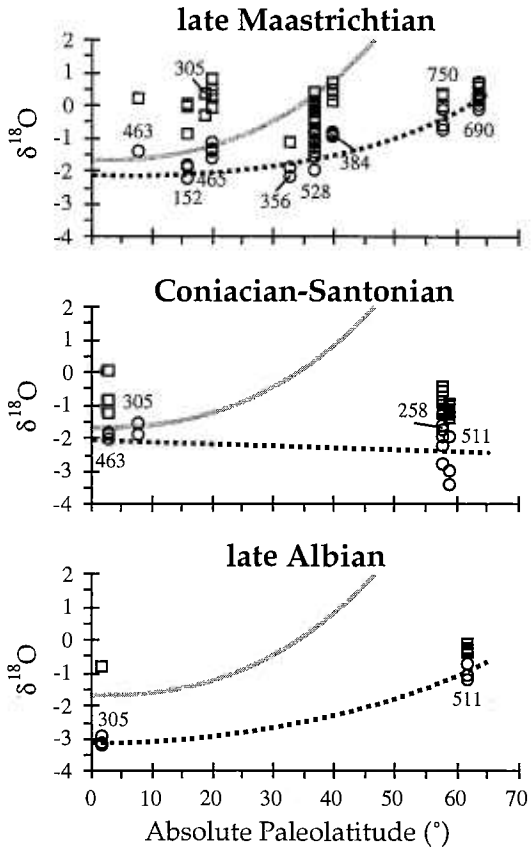

Figure 11. Uncorrected oxygen isotope values for surface-dwelling planktonic foraminifera and benthic foraminifera from bathyal depths plotted against absolute paleolatitude for each site during the late Albian, Coniacian–Santonian, and late Maastrichtian. Shaded curve represents the mean Holocene $\delta^{18}O$ gradient based on analysis of planktonic foraminifera occurring in core tops (after Savin et al., 1985). Dashed line is a best-fit curve through all surface-water $\delta^{18}O$ values except for late Maastrichtian values from Sites 305 and 463, which are suspected of having been diagenetically altered. See text for sources of data.

Zachos et al. (1994) used the following third-order polynomial to calculate a $\delta^{18}O$ adjustment factor for isotopic analyses that compensates for changes in surface waters at different latitudes based on modern latitudinal changes in δ_w related latitudinal salinity gradients in the modern:

$$y = 0.576 + 0.04x - 0.0017x^2 + 1.35 \cdot 10^{-5}x^3 \qquad (2)$$

(y represents the difference in δ_w from an isohaline ocean, x represents latitude from 0°–70°). To adjust for salinity, y is subtracted from the observed surface-dwelling planktonic foraminiferal $\delta^{18}O$ values. By doing so, low-latitude $\delta^{18}O$ values decrease by as much as 0.8‰, whereas high-latitude values become heavier by <0.1‰.

This approach was used with the Cretaceous planktonic foraminiferal $\delta^{18}O$ dataset by averaging the $\delta^{18}O$ values of surface-dwelling species from each site, then subtracting the adjustment factors for each paleolatitude. Plots of the averaged uncorrected and corrected $\delta^{18}O$ values from surface-dwelling planktonics are illustrated in Figure 12 with the corrected Holocene planktonic foraminiferal $\delta^{18}O$ sea-surface temperature curve for reference. As a result of this adjustment, the slopes of the latitudinal thermal gradient curves increase for the late Albian and late Maastrichtian time intervals, and become nearly horizontal, rather than negative, for the Coniacian–Santonian. Late Albian sea-surface $\delta^{18}O$ values that are adjusted for modern-day salinity gradients are 3.8‰ (≈30 °C) in the tropics and −0.8‰ (≈16 °C) in the high latitudes. Adjusted sea-surface $\delta^{18}O$ values in the Coniacian–Santonian interval are about −2.6‰ (≈24 °C) in the tropics and range between −2.0‰ and −2.6‰ (21–24 °C) in the high latitudes; essentially there was no latitudinal thermal gradient. In the late Maastrichtian, the adjusted $\delta^{18}O$ values indicate that tropical surface waters were about −2.8‰ (≈25 °C) at Site 152, while high-latitude values averaged ≈0.5‰ (≈11 °C).

Even with the salinity adjustments, it appears that sea-surface temperatures are still underestimated in the tropics and may be overestimated in the high latitudes, particularly for Coniacian–Santonian time. In the absence of visible evidence for shell recrystallization or secondary calcite overgrowths in the Turonian and younger Cretaceous foraminifera from Site 511, we assume measured $\delta^{18}O$ values approximate equilibrium fractionation, but we continue to worry about "invisible" diagenesis. We do suspect that diagenesis affected the isotopic results from Sites 305 and 463 as the $\delta^{18}O$ values from these sites are lower than $\delta^{18}O$ values from modern tropical planktonic foraminifera.

A second possible problem with calculating latitudinal thermal gradients is that corrections based on the present may be inadequate for the Cretaceous. During the Cretaceous the poleward atmospheric and oceanic transport of heat was probably greater than at present (Barron and Washington, 1982; Barron, 1987; Rind and Chandler, 1991; Barron et al., 1993, in press), and the mode of deep-water circulation may have been different from today with formation of warm saline deep water in the tropics and subtropics (Brass et al., 1982). These differences would have influenced the salinity and oxygen isotopic gradients in contemporary oceans. If the salinity and $\delta^{18}O$ differences between the low- and high-latitude surface oceans were enhanced during portions of the Cretaceous, then salinity corrections based on modern observations would result in underestimation of low-latitude temperatures and overestimation of high-latitude temperatures.

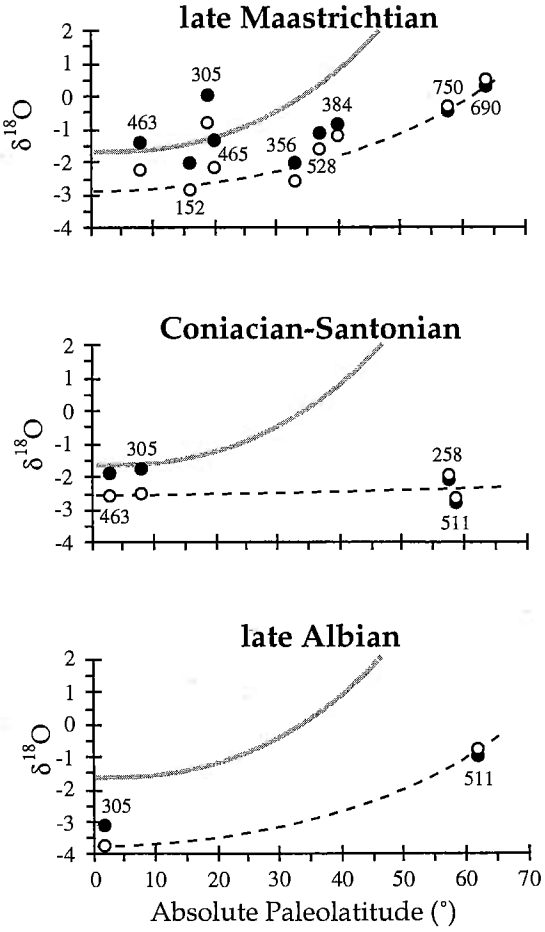

Figure 12. Oxygen isotope values for surface-dwelling planktonic foraminifera plotted against paleolatitude. The $\delta^{18}O$ data include values shown as solid circles, which represent averaged upper surface-water values for each site (from Fig. 11), and hollow circles, which represent averaged surface-water values that have been adjusted for meridional heterogeneities in salinity using the third-order polynomial of Zachos et al. (1994). The stippled curve represents the salinity-corrected Holocene $\delta^{18}O$ gradient mean based on analysis of planktonic foraminifera occurring in core tops (after Savin et al., 1985). Dashed line is a best-fit curve through all corrected surface-water $\delta^{18}O$ values except for the late Maastrichtian values from Sites 305 and 463, which are suspected of having been diagenetically altered.

Intermediate-Water Latitudinal Isotopic Differences

The benthic $\delta^{18}O$ values shown in Figures 10 and 11 record the isotopic composition of water that bathed the sediment/water interface at lower to upper bathyal depths and, thus, can be used to characterize paleotemperature changes of intermediate water masses relative to latitude and time. Our results indicate that the tropical benthic isotopic paleotemperatures were slightly warmer at low latitudes than at high latitudes during the late Albian and late Maastrichtian. Assuming that the salinity of middle–Late Cretaceous intermediate water masses was normal and diagenetic alteration of the benthic foraminifera was minimal, the paleotempera-

ture of late Albian intermediate waters is estimated at 14 °C at high latitudes, whereas late Albian tropical intermediate waters were ≈16 °C. During Turonian–early Campanian time, high-latitude deep waters were significantly warmer, ranging between ≈16 and 19 °C, while low-latitude deep waters were no warmer than ≈18 °C. Intermediate waters cooled particularly in the high latitudes by the late Maastrichtian, with values from Site 690 of ≈10 °C and low-latitude intermediate waters ranging between 10 and 16 °C. As discussed earlier, the $\delta^{18}O$ values from tropical foraminifera, particularly at Sites 463 and 305, may have been diagenetically altered, resulting in an underestimation of water paleotemperatures.

The only isotopic study of biogenic calcite from deeper water depths is that of Barron and Saltzman (1982), who analyzed Coniacian–late Campanian inoceramids from Hole 530A in the Angola Basin, which was ≈4000 m deep during the Late Cretaceous. Extremely warm paleotemperatures were found in one sample from the Coniacian (≈22 °C) and another from the upper Campanian (≈18 °C), while the remaining Campanian paleotemperatures were as cool or cooler than intermediate waters of the same age (Fig. 1). Barron and Saltzman (1982) theorized that such light oxygen isotopic values at abyssal depths could only have originated from a plume of warm, dense, saline water that sank from the shelf off northwestern Africa and into the Angola Basin. These authors also argued that the high latitudes served as a source of deep water in the Pacific based on the relatively high $\delta^{18}O$ values that were obtained from benthic foraminifera at Site 305. Results of general circulation model experiments (Barron and Peterson, 1990) also predict multiple sources of deep water during the middle Cretaceous, with regions of the polar Pacific and eastern Tethys identified as possible source areas.

Woo et al. (1992) provided additional support for a Tethyan source of deep-water formation. Analyses of well-preserved mollusks and radial calcite cement from Albian–Cenomanian limestones yielded $\delta^{18}O$ values between −0.5‰ and −2.9‰, which is as much as 2.5‰ higher than expected from temperature alone if Cretaceous surface waters were at least as warm as in the modern. Assuming the $\delta^{18}O$ values reflect a salinity effect, these authors determined that surface waters in the Gulf Coast region were sufficiently dense to have acted as a significant component of deep-water formation during the middle Cretaceous.

Kauffman and Johnson (1988) have recognized a core tropical climate zone during the middle Cretaceous that they termed *Supertethys*, based on paleontological and geological evidence for exceptional warmth during the Cenomanian and Turonian. These authors suggested that Supertethys would have served as a major source for warm saline deep water in the tropical belt until Maastrichtian time (Johnson and Kauffman, in press).

By Maastrichtian time, the south polar region may have been an important source of deep-water formation. Oxygen isotope analyses of foraminifera from nearshore sections in the Antarctic Peninsula (Barrera et al., 1987) indicate that shelfal waters were between 4 and 10 °C, which is within the range of Maastrichtian deep-sea benthic $\delta^{18}O$ at Site 305 (Douglas and Savin, 1975). This is supported by the cool planktonic foraminiferal values that were obtained from Site 690 on the other side of the Weddell Sea basin (Barrera and Huber, 1990). Perhaps the high-latitude cooling that began during the middle Campanian initiated a transition from a predominantly low-latitude source of deep waters to a dominantly high-latitude source (MacLeod, 1994). Recovery of isotopically well-preserved benthic foraminiferal $\delta^{18}O$ values from Upper Cretaceous deep-sea sequences across a wide range of paleodepths and latitudes will be essential to test this hypothesis.

Global Paleotemperature Estimates

The late Campanian–Maastrichtian surface-water cooling observed in the southern high latitudes (Fig. 11) was not a local effect, as it has been identified at several shallow-water and deep-sea sites in the southern high latitudes (Barrera et al., 1987; Barrera and Huber, 1990; Pirrie and Marshall, 1990; Ditchfield et al., 1994; Huber and Boersma, 1994; this study) as well as several sites in the middle latitudes of both hemispheres (e.g., Saito and Van Donk, 1974; Boersma and Shackleton, 1981; Boersma, 1984; D'Hondt and Lindinger, 1994). Given the excellent preservation and consistent taxonomic order of stable isotopic signatures, we do not believe that the strongly negative $\delta^{18}O$ values found in the Turonian–early Campanian at Site 511 are a diagenetic artifact, particularly because $\delta^{18}O$ determinations from Site 258 and the Antarctic Peninsula (Ditchfield et al., 1994) yield results that are compatible with the Site 511 record. Nonetheless, these data are not entirely consistent with some isotopic paleotemperature studies for the middle–Late Cretaceous.

A variety of Cretaceous paleotemperature curves have been derived from $\delta^{18}O$ analyses of belemnite rostra. Warming maxima have been recognized in the Albian and Coniacian–Santonian in Europe and the southeastern United States (Lowestam and Epstein, 1954), Albian–Cenomanian in northwest Germany (Spaeth et al., 1971), Coniacian–Santonian in New Zealand (Stevens and Clayton, 1971), and late Albian–Cenomanian and late Maastrichtian in the Russian Platform and adjacent areas (Naydin et al., 1966); however, pronounced variance of belemnite $\delta^{18}O$ values from the same stratigraphic unit (e.g., Lowenstam and Epstein, 1954; Spaeth et al., 1971) and geochemical studies (Veizer, 1974) indicate that the paleotemperature signal in belemnites is often overprinted by the $\delta^{18}O$ from secondary calcite. Thus, these older belemnite paleotemperature estimates may be unreliable.

More trustworthy paleotemperature data have been derived from oxygen isotopic analyses of fish teeth from the Cretaceous of Israel (Kolodny and Raab, 1988). The $\delta^{18}O$ signal preserved in phosphate is considered less prone to diagenetic alteration than in skeletal calcite. These data provide a record of temperature changes at relatively coarse sampling intervals from the Berriasian through early Eocene for shallow water in the eastern Tethys Sea, (≈10°N paleolatitude). Results of Kolodny and Raab's (1988) investigation indicate that maximum temperatures occurred near the Cenomanian–Turonian boundary, with shelfal marine temperatures reaching 32–33 °C. This maximum was followed by a cooling to ≈20 °C during the Maastrichtian.

As noted earlier, the isotopic values obtained from tropical Pacific Sites 305 and 463 are suspected of having been diagenetically altered and, therefore, paleotemperature estimates from these sites may be unreliable. Nonetheless, the long-term trends in the tropical surface-water paleotemperatures are consistent with our high-latitude results, showing maximum warmth during the middle Cretaceous and coolest temperatures during the late Maastrichtian.

Jenkyns et al. (1994) provided a high-resolution record of oxygen and carbon isotope values in Upper Cretaceous chalk sequences in the south and east coast of England and in a middle–Upper Cretaceous pelagic limestone sequence in the Bottaccione Gorge of Gubbio, Italy. All of the isotopic data presented in their study were

obtained from analyses of whole rock samples. The East Kent section, which ranges from the lower Cenomanian through the lowermost Campanian, contains a minor amount of calcite cement and is considered the best preserved of the studied sequences. The $\delta^{18}O$ data from that section show values in the range of about −3.0‰ during the early Cenomanian, increasing to about −2.0‰ by middle Cenomanian, then decreasing through the late Cenomanian with lightest values of about −3.8‰ during the earliest Turonian. Progressively increasing $\delta^{18}O$ values follow from the middle Turonian into the earliest Campanian. The Bottacione Gorge data reveal a remarkably similar curve, even though the values tend to be ≈0.5‰ lower than at East Kent, and show considerably more variance. Although Jenkyns et al. (1994) concede that the absolute $\delta^{18}O$ values may be slightly offset because of diagenetic factors, they consider the English Chalk and Bottacione Gorge $\delta^{18}O$ curves to reflect global changes in marine paleotemperatures, with the Cenomanian/Turonian boundary denoting a major climatic turning point.

Sellwood et al. (1994) have reported sea-surface temperature estimates for the late Albian, Cenomanian, and early Turonian based on their own oxygen isotopic analyses of planktonic foraminifera from several Atlantic and Pacific low- to middle-latitude DSDP sites, and from previously published $\delta^{18}O$ analyses of middle- to high-latitude belemnites. These authors concluded that the minimum mean tropical temperatures were close to present-day values and that polar temperatures were close to 0 °C. This suggests a considerably higher latitudinal thermal gradient than the reconstructions in Figures 11 or 12 would indicate; however, the polar temperatures cited in the Sellwood et al. (1994) study are based entirely on poleward extrapolation of a best-fit curve through the belemnite data. As discussed above, as well as in the Sellwood et al. (1994) article, belemnites are very susceptible to diagenesis, and their paleoecology is not well understood. We therefore do not consider the Sellwood et al. (1994) 0 °C estimate of middle Cretaceous polar temperatures to be a viable alternative to our high-latitude results.

In summary, the most reliable oxygen isotope data that span middle–Late Cretaceous time indicate that maximum Cretaceous warming occurred during the earliest Turonian, when global sea level was higher than at any other time during the Mesozoic Era (e.g., Hancock and Kauffman, 1979; Haq et al., 1988; Fig. 1) and when there was a dramatic increase in the volume of organic carbon buried in marine basins worldwide (e.g., Arthur et al., 1985, 1987; Fig. 1); however, the climate record immediately following the earliest Turonian ultrathermal is less clear. Isotopic paleotemperatures from the high latitudes suggest that very warm surface-water temperatures persisted from Turonian through early Campanian time, whereas several studies from the low and middle latitudes of the Northern Hemisphere indicate that a long-term cooling immediately followed the ultrathermal event. It is not apparent why there is such a discrepancy in these paleotemperature trends, as the differences are too significant to be explained by sampling or correlation problems. Further investigation of the Cretaceous stable isotope record and other climatic proxies will be essential to develop a better understanding of this extreme period of global warmth.

CLIMATIC IMPLICATIONS

The oxygen isotopic data from DSDP Sites 511, 327, and 258 reveal exceptionally warm sea-surface temperatures in the southern high latitudes during the middle–Late Cretaceous and apparently very low to nonexistent latitudinal thermal gradients. As a horizontal thermal gradient across latitudes seems implausible for any period in geologic history, it is likely that our assumptions about the $\delta^{18}O$ of Cretaceous water are invalid and that some of the isotopic values, particularly in low latitudes, have been diagenetically altered. Despite these problems, the isotopic preservation at each of the high-latitude sites is judged to be good, and there is ample independent evidence for high-latitude warmth during the middle–Late Cretaceous.

These results amplify the need to understand what forcing mechanisms could have produced such warm polar temperatures. Some factors that have been suggested include (1) changes in land-sea distributions (Barron et al., 1980, 1981; Barron, 1983; Barron and Washington, 1982), (2) increased levels of CO_2 in the atmosphere (Barron and Washington, 1984; Schneider et al., 1985; Barron and Washington, 1985; Berner, 1991), and (3) increased efficiency of atmospheric and oceanic heat transport (e.g., Barron and Washington, 1982; Rind and Chandler, 1991; Barron et al., 1993b). Results from a series of climate sensitivity experiments (Barron and Washington, 1984, 1985; Barron et al., 1993a) suggested that Cretaceous land-sea distributions together with four times present-day atmospheric CO_2 concentrations could increase globally averaged surface temperatures by ≈8 °C, which is within the temperature range estimated for the Albian based on the geologic record; however, the response of the climate models to increased levels of atmospheric CO_2 was to raise tropical temperatures while increasing polar warmth, resulting in equator-to-pole thermal gradients that were too high.

Several general circulation model experiments have demonstrated that the oceans play an important role in maintaining warm climates with low equator-to-pole temperatures. Rind and Chandler (1991) determined that a 15% increase in poleward ocean heat transport led to removal of polar sea ice and a globally averaged temperature that was 2 °C warmer than in a present-day control experiment. These results were corroborated by Barron et al. (1993b), who, in a series of general circulation model studies using Cretaceous geography, demonstrated that a small increase in ocean heat transport resulted in a significant increase in polar temperatures and a decline in tropical temperatures. More recently, Barron et al. (in press) have determined that middle Cretaceous surface-water temperatures averaging 6.2° C warmer than the present could be achieved in general circulation model experiments using Cretaceous geography, four times present pCO_2, and a 1.2×10^{15} W/m^2 increase in poleward heat transport. A globally averaged temperature of 6 °C for surface waters, however, represents a minimum estimate for the Albian, with mean annual surface temperatures of ≈0 °C at the poles and ≈27 °C in the tropics (Barron et al., in press). On the other hand, our paleotemperature estimates for surface waters at ≈60°S paleolatitude average ≈15 °C for the Albian and ≈24 °C for the Coniacian–Santonian, even with a salinity adjustment.

General circulation model experiments have vastly improved in their capability to simulate the warm climates of the Cretaceous since ocean heat flux has been incorporated as a variable. But in order to simulate a warm Cretaceous climate with polar temperatures as warm as our study suggests, the general circulation models will probably need to increase in complexity and assume a greater amount of poleward ocean heat flux. The GENESIS model used by Barron et al. (1993b, in press) assumes a two-layer ocean with a 50 m

mixed layer slab and a "control" value for ocean heat transport that was developed based on a best fit with modern observations, which is only 15% of the ocean heat transport calculated by Carissimo et al. (1985); however, warm, saline plumes probably sank below the surface mixed layer at low latitudes during the Cretaceous and resurfaced at high latitudes. These halothermal circulation cells would have provided a major conduit for poleward heat transport and would have contributed to maintaining low equator-to-pole thermal gradients.

Evidence for increased warm saline deep-water production during the middle Cretaceous has been cited by Sliter (in press) based on the widespread occurrence of hiatuses in upper Albian, lower–middle Cenomanian, Turonian, and lower Santonian pelagic carbonate sequences worldwide. On the other hand, high-latitude cooling and paleogeographic changes, such as the opening of circum-Antarctic gateways, may have caused major hiatuses that have been observed in the middle Campanian and the upper Maastrichtian (Huber and Watkins, 1992; Sliter, in press). The timing and duration of these hiatuses are not well constrained, however, because of poor age control in many sections.

The need for much additional information on Cretaceous climate is clearly demonstrated in this study, as confirmation that the oxygen isotope trends we have observed at high latitudes reflect a global climatic temperature signal will require verification using other paleoclimatic proxies from marine and terrestrial sections. But even considering greater equator-to-pole differences in surface-water salinity, our results indicate higher surface temperatures at austral high latitudes than previous studies have suggested. The challenge for future studies is to determine how the Earth could have maintained such a warm climate with such low equator-to-pole temperature differences.

ACKNOWLEDGMENTS

This research benefited from discussions with Ken MacLeod, Jim Pospichal, Dave Watkins, Jim Zachos, and Tom Crowley and reviews by Tim Bralower, Ken MacLeod, Bill Sliter, and Eric Barron. We thank Paul Fullager for analyzing strontium isotope samples from Site 511 and My Le Ducharme for help with computer graphics. This work was supported by a grant from the Smithsonian Institution's Scholarly Studies Program.

REFERENCES CITED

Arthur, M. A., Hinga, K. R., Pilson, M. E., Whitaker, D., and Allard, D., 1991, Estimates of pCO_2 for the last 120 Ma based on the ^{13}C of marine phytoplankton organic matter: EOS (American Geophysical Union Transactions), v. 72, p. 166.

Arthur, M. A., Schlanger, S. O., and Jenkyns, H. C., 1987, The Cenomanian–Turonian oceanic anoxic event, II. Palaeoceanographic controls on organic-matter production and preservation, *in* Brooks, J., and Fleet, A. J., eds., Marine petroleum source rocks: Geological Society of London Special Publication 26, p. 401–420.

Barnard, P., 1973, Mesozoic floras, *in* Hughes, N., ed., Organisms and continents through time: Palaeontological Association of London Special Papers in Palcontology, no. 12, p. 175–188.

Barrera, E., and Huber, B. T., 1990, Evolution of Antarctic waters during the Maestrichtian: Foraminifer oxygen and carbon isotope ratios, ODP Leg 113, *in* Barker, P. F., Kennett, J. P., et al., Proceedings of the Ocean Drilling Program, scientific results: College Station, Texas, Ocean Drilling Program, v. 113, p. 813–823.

Barrera, E., Huber, B. T., Savin, S. M., and Webb, P. N., 1987, Antarctic marine temperatures: Late Campanian through early Paleocene: Paleoccanography, v. 2, p. 21–47.

Barron, E. J., 1983, A warm, equable Cretaceous: The nature of the problem: Earth Science Reviews, v. 19, p. 305–338.

Barron, E. J., 1987, Global Cretaceous paleogeography—International Geologic Correlation Programme Project 191: Palaeogeography, Palaeoclimatology, Palaeoecology, v. 59, p. 207–216.

Barron, E. J., and Peterson, W. H., 1990, Mid-Cretaceous ocean circulation: Results from model sensitivity studies: Paleoccanography, v. 5, p. 319–337.

Barron, E. J., and Washington, W. M., 1982, Cretaceous climate: A comparison of atmospheric simulations with the geologic record: Palaeogeography, Palaeoclimatology, Palaeoecology, v. 40, p. 103–133.

Barron, E. J., and Washington, W. M., 1984, The role of geographic variables in explaining paleoclimates: Results from Cretaceous climate model sensitivity studies: Journal of Geophysical Research, v. 89, p. 1267–1279.

Barron, E. J., and Washington, W. M., 1985, Warm Cretaceous climates: High atmospheric CO_2 as a plausible mechanism, *in* Sundquist, E. T., and Broecker, W. S., eds., The carbon cycle and atmospheric CO_2: Natural variations Archean to present: American Geophysical Union Geophysical Monograph 32, p. 546–553.

Barron, E. J., Sloan, J. L., and Harrison, C. G. A., 1980, Potential significance of land-sea distribution and surface albedo variations as a climatic forcing factor; 180 m.y. to the present: Palaeogeography, Palaeoclimatology, Palaeoecology, v. 30, p. 17–40.

Barron, E. J., Thompson, S. L., and Schneider, S. H., 1981, An ice-free Cretaceous? Results from climate model simulations: Science, v. 212, p. 501–508.

Barron, E. J., Fawcett, P. J., Pollard, D., and Thompson, S., 1993a, Model simulations of Cretaceous climates: The role of geography and carbon dioxide: Royal Society of London Philosophical Transactions, ser. B, v. 341, p. 307–316.

Barron, E. J., Peterson, W. H., Pollard, D., and Thompson, S., 1993b, Past climate and the role of ocean heat transport: Model simulations for the Cretaceous: Paleoccanography, v. 8, p. 785–798.

Barron, E. J., Fawcett, P. J., Petersen, W. H., Pollard, D., and Thompson, S. T., in press, A "simulation" of mid-Cretaceous climate: Paleoceanography.

Basov, I. A., and Krasheninnikov, V. A., 1983, Benthic foraminifers in Mesozoic and Cenozoic sediments of the southwestern Atlantic as an indicator of paleoenvironment, Deep Sea Drilling Project Leg 71, *in* Ludwig, W. J., Krasheninnikov, V. A., et al., Initial reports of the Deep Sea Drilling Project: Washington, D.C., U.S. Government Printing Office, v. 71, p. 739–787.

Bé, A. W. H., 1977, An ecological, zoogeographic and taxonomic review of recent planktonic foraminifera, *in* Ramsay, A. T. S., ed., Oceanic micropalaeontology 1: London, United Kingdom, Academic Press, p. 1–100.

Berger, W. H., 1971, Planktonic foraminifera: Sediment production in an oceanic front: Journal of Foraminiferal Research, v. 1, p. 95–118.

Berner, R. A., 1991, A model for atmospheric CO_2 over Phanerozoic time: American Journal of Science, v. 291, p. 339–376.

Boersma, A., 1984, Campanian through Paleocene paleotemperature and carbon isotope sequence and the Cretaceous-Tertiary boundary, *in* Berggren, W. A., and Van Couvering, J. A., eds., Catastrophes and Earth history: Princeton, New Jersey, Princeton University Press, p. 247–277.

Boersma, A., and Premoli Silva, I., 1989, Atlantic Paleogene biserial heterohelicid foraminifera and oxygen minima: Paleoceanography, v. 4, p. 271–286.

Boersma, A., and Shackleton, N. J., 1981, Oxygen and carbon isotope variations and planktonic foraminiferal depth habitats: Late Cretaceous to Paleocene, central Pacific, DSDP Sites 463 and 465, Leg 65, *in* Thiede, J., Vallier, T. L., et al., Initial reports of the Deep Sea Drilling Project: Washington, D.C., U.S. Government Printing Office, v. 65, p. 513–526.

Bralower, T. J., 1992, Aptian–Albian calcareous nannofossil biostratigraphy of ODP Site 763 and the correlation between high- and low-latitude zonations, *in* Kidd, R. B., and Rea, D. K., eds., Synthesis of results from scientific drilling in the Indian Ocean, American Geophysical Union Geophysical Monograph 70, p. 245–252.

Bralower, T. J., Sliter, W. V., Arthur, M. A., Leckie, R. M., Allard, D., and Schlanger, S. O., 1993, Dysoxic/anoxic episodes in the Aptian–Albian (Early Cretaceous), *in* Pringle, M. S., Sager, W. W., Sliter, W. V., and Stein, S., eds., The Mesozoic Pacific: Geology, tectonics, and volcanism 77: American Geophysical Union Monograph v. 77, p. 5–37.

Brass, G. W., Southam, J. R., and Peterson, W. H., 1982, Warm saline bottom water in the ancient ocean: Nature, v. 296, p. 620–623.

Broecker, W. S., 1986, Oxygen isotope constraints on surface ocean temperatures: Quaternary Research, v. 26, p. 131–134.

Carissimo, B. C., Oort, A. H., and Voner Haar, T. H., 1985, Estimating the meridional energy transports in the atmosphere and ocean: Journal of Physical Oceanography, v. 15, p. 82–91.

Caron, M., and Homewood, P., 1983, Evolution of early planktonic foraminifera: Marine Micropaleontology, v. 7, p. 453–462.

Ciesielski, P. F., Kristoffersen, Y., et al., 1988, Proceedings of the Ocean Drilling Program, initial reports: College Station, Texas, Ocean Drilling Program, v. 114, 815 p.

Colbert, E. H., 1973, Continental drift and the distribution of fossil reptiles, *in* Tarling, D. H., and Runcorn, S. K., eds., Implications of continental drift to the earth sciences: New York, Academic Press, p. 395–412.

Corfield, R. M., and Cartlidge, J. E., 1991, Isotopic evidence for the depth stratification of fossil and Recent Globigerinina: Historical Biology, v. 5, p. 37–63.

Corfield, R. M., Hall, M. A., and Brasier, M. D., 1990, Stable isotope evidence for foraminiferal habitats during the development of the Cenomanian/Turonian oceanic anoxic event: Geology, v. 18, p. 175–178.

Crowley, T. J., and North, G. R., 1991, Paleoclimatology: Oxford, United Kingdom, Oxford University Press, 339 p.

Davies, T. A., and Luyendyk, B. P., 1974, Initial reports of the Deep Sea Drilling Project: Washington, D.C., U.S. Government Printing Office, v. 26, 1129 p.

Deuser, W. G., Hemleben, C., and Spindler, M., 1981, Seasonal changes in species composition, numbers, size, mass, and isotopic composition of planktonic foraminifera settling into the deep Sargasso Sea: Palaeogeography, Palaeoclimatology, Palaeoccology, v. 33, p. 103–127.

D'Hondt, S., and Arthur, M. A., 1995, Interspecific variation in stable isotopic signals of Maestrichtian planktonic foraminifera: Paleoceanography, v. 10, p. 125–135.

D'Hondt, S., and Lindinger, M., 1994, A Maestrichtian stable isotopic record and its paleoceanographic implications: South Atlantic DSDP Site 528: Palaeogeography, Palaeoclimatology, Palaeoecology, v. 112, p. 363–378.

Ditchfield, P. W., Marshall, J. D., and Pirrie, D., 1994, High latitude palaeotemperature variation: New data from the Tithonian to Eocene of James Ross Island, Antarctica: Palaeogeography, Palaeoclimatology, Palaeoecology, v. 107, p. 79–101.

Douglas, R. G., 1969, Upper Cretaceous planktonic foraminifera in northern California: Micropaleontology, v. 15, p. 151–209.

Douglas, R. G., and Savin, S. M., 1973, Oxygen and carbon isotope analyses of Cretaceous and Tertiary foraminifera from the central North Pacific, *in* Winterer, E. L., Ewing, J. I., et al., Initial reports of the Deep Sea Drilling Project 17: Washington, D.C., U.S. Government Printing Office, p. 591–607.

Douglas, R. G., and Savin, S. M., 1975, Oxygen and carbon isotope analyses of Tertiary and Cretaceous microfossils from the Shatsky Rise and other sites in the North Pacific Ocean, *in* Initial reports of the Deep Sea Drilling Project: Washington, D.C., U.S. Government Printing Office, v. 32, p. 509–520.

Douglas, R. G., and Savin, S. M., 1978, Oxygen isotopic evidence for the depth stratification of Tertiary and Cretaceous foraminifera: Palaeogeography, Palaeoclimatology, Palaeoecology, v. 3, p. 175–196.

Emiliani, C., 1954, Depth habitats of some species of pelagic foraminifera as indicated by oxygen isotope ratios: American Journal of Science, v. 252, p. 149–158.

Fairbanks, R. G., and Wiebe, P. H., 1980, Foraminifera and chlorophyll maximum: Vertical distribution, seasonal succession, and paleoceanographic significance: Science, v. 209, p. 1524–1525.

Fairbanks, R. G., Sverdlove, R. F., Wiebe, P. H., and Bé, A. W. H., 1982, Vertical distribution and isotopic fractionation of living planktonic foraminifera from the Panama Basin: Nature, v. 298, p. 841–844.

Frakes, L. A., 1986, Mesozoic–Cenozoic climate history and causes of the glaciation, *in* Hsü, K. J., ed., Mesozoic and Cenozoic oceans: American Geophysical Union Geodynamics Series, v. 15, p. 33–48.

Frakes, L. A., Francis, J. E., and Syktus, J. I., 1992, Climate modes of the Phanerozoic: Cambridge, United Kingdom, Cambridge University Press, 274 p.
Frederiksen, N. O., 1989, Changes in floral diversities, floral turnover rates, and climates in Campanian and Maastrichtian time, North Slope of Alaska: Cretaceous Research, v. 10, p. 249–266.
Garrison, R. E., 1981, Diagenesis of oceanic carbonate sediments: A review of the DSDP perspective: Society of Economic Paleontologists and Mineralogists Special Publication 32: p. 181–207.
Gieskes, J. M., 1981, Deep-sea drilling interstitial water studies: Implications for chemical alteration of the oceanic crust, layers I and II, *in* Warme, J. E., Douglas, R. G., and Winterer, E. L. eds., The Deep Sea Drilling Project: A decade of progress: Society of Economic Paleontologists and Mineralogists Special Publication 32, p. 149–168.
Gieskes, J. M., and Lawrence, J. R., 1981, Alteration of volcanic matter in deep sea sediments: Evidence from the chemical composition of interstitial waters from deep sea drilling cores: Geochimica et Cosmochimica Acta, v. 45, p. 1687–1703.
Gordon, W. A., 1973, Marine life and ocean surface currents in the Cretaceous: Journal of Geology, v. 81, p. 269–284.
Gradstein, F. M., Agterberg, F. P., Ogg, J. G., Hardenbol, J., van Veen, P., Thierry, J., and Huang, Z., 1994, A Mesozoic time scale: Journal of Geophysical Research, v. 99, p. 24051–24074.
Habicht, J. K. A., 1979, Paleoclimate, paleomagnetism, and continental drift: Tulsa, Oklahoma, American Association of Petroleum Geologists Studies in Geology, no. 9, p. 1–31.
Hancock, J. M., and Kauffman, E. G., 1979, The great transgressions of the Late Cretaceous: Journal of the Geological Society of London, v. 136, p. 175–186.
Haq, B. U., Hardenbol, J., and Vail, P. R., 1988, Mesozoic and Cenozoic chronostratigraphy and cycles of sea level change, *in* Wilgus, C. K., Hastings, B. S., Posamentier, H., van Wagoner, J., Ross, C. A., and Kendall, C. G. S., eds., Sea level changes: An integrated approach: Society of Economic Paleontologists and Mineralogists Special Publication 42, p. 71–108.
Hart, M. B., 1980, A water depth model for the evolution of the planktonic Foraminiferida: Nature, v. 286, p. 252–254.
Hart, M. B., and Bailey, H. W., 1979, The distribution of planktonic Foraminiferida in the mid-Cretaceous of NW Europe: International Union of Geological Sciences, ser. A, Aspekte der Kreide Europas, v. 6, p. 527–542.
Hemleben, C., Spindler, M., and Anderson, O. R., 1989, Modern planktonic foraminifera: New York, Springer-Verlag, 335 p.
Herb, R., 1974, Cretaceous planktonic foraminifera from the eastern Indian Ocean, *in* Davies, T. A., Luyendyk, B. P., et al., Initial reports of the Deep Sea Drilling Project: Washington, D.C., U.S. Government Printing Office, v. 26, p. 745–769.
Huber, B. T., 1990, Maestrichtian planktonic foraminifer biostratigraphy of the Maud Rise (Weddell Sea, Antarctica): ODP Leg 113 holes 689B and 690C, *in* Barker, P. F., Kennett, J. P., et al., Proceedings of the Ocean Drilling Program, scientific results 113: College Station, Texas, Ocean Drilling Program, p. 489–513.
Huber, B. T., 1992, Upper Cretaceous planktonic foraminiferal biozonation for the Austral Realm: Marine Micropaleontology, v. 20, p. 107–128.
Huber, B. T., and Boersma, A., 1994, Cretaceous origination of *Zeauvigerina* and its relationship to Paleocene biserial planktonic foraminifera: Journal of Foraminiferal Research, v. 24, p. 268–287.
Huber, B. T., and Watkins, D. K., 1992, Biogeography of Campanian–Maastrichtian calcareous plankton in the region of the Southern Ocean: Paleogeographic and paleoclimatic implications, *in* Kennett, J. P., and Warnke, D. A., eds., The Antarctic paleoenvironment: A perspective on global change: American Geophysical Union Antarctic Research Series, v. 56, p. 31–60.
Jenkyns, H. C., Gale, A. S., and Corfield, R. M., 1994, Carbon- and oxygen-isotope stratigraphy of the English Chalk and Italian Scaglia and its palaeoclimatic significance: Geological Magazine, v. 131, p. 1–34.
Johnson, C. C., and Kauffman, E. G., in press, Maastrichtian extinction patterns of Caribbean Province rudistids, *in* MacLeod, N., and Keller, G., eds., Biotic and environmental effects of the Cretaceous-Tertiary boundary event: New York, W. W. Norton and Co.
Johnson, K. R., and Hickey, L. J., Patterns of megafloral change across the Cretaceous-Tertiary boundary in the northern Great Plains and Rocky Mountains, *in* Sharpton, V. L., and Ward, P. D., eds., Global catastrophes in Earth history; An interdisciplinary conference on impacts, volcanism, and mass mortality: Geological Society of America Special Paper 247, p. 433–444.
Jones, C. E., Jenkyns, H. C., Coe, A. L., and Hesselbo, S. P., 1994, Strontium isotopic variations in Jurassic and Cretaceous seawater: Geochimica et Cosmochimica Acta, v. 58, p. 3061–3074.
Kauffman, E. G., 1973, Cretaceous Bivalvia, *in* Hallam, A., ed., Atlas of paleobiogeography: Amsterdam, Netherlands, Elsevier, p. 351–383.
Kauffman, E. G., and Johnson, C. C., 1988, The morphological and ecological evolution of middle and Upper Cretaceous reef-building rudistids: Palaios, v. 3, p. 194–216.
Kolodny, Y., and Raab, M., 1988, Oxygen isotopes in phosphatic fish remains from Israel: Paleothermometry of tropical Cretaceous and Tertiary shelf waters: Palaeogeography, Palaeoclimatology, Palaeoecology, v. 64, p. 59–67.
Krasheninnikov, V. A., and Basov, I. A., 1974, Cenozoic planktonic foraminifers of the Falkland Plateau and Argentine Basin, Deep Sea Drilling Project Leg 71, *in* Ludwig, W. J., Krasheninnikov, V. A., et al., Initial reports of the Deep Sea Drilling Project: Washington, D.C., U.S. Government Printing Office, v. 71, p. 821–858.
LaBrecque, J. L., editor, 1986, South Atlantic Ocean and adjacent continental margin atlas 13: Woods Hole, Massachusetts, Ocean Margin Drilling Program Regional Atlas Series, no. 13, 21 p.
Lawrence, J. R., Drever, J. I., Anderson, T. F., and Brueckner, H. K., 1979, Importance of volcanic alteration in the sediments of Site 323: Chemistry, $^{18}O/^{16}O$, $^{87}Sr/^{86}Sr$: Geochimica et Cosmochimica Acta, v. 43, p. 573–588.
Leckie, R. M., 1987, Paleoecology of mid-Cretaceous planktonic foraminifera: A comparison of open ocean and epicontinental sea assemblages: Micropaleontology, v. 33, p. 164–176.
Lloyd, C. R., 1982, The mid-Cretaceous earth: Paleogeography, ocean circulation and temperature, atmospheric circulation: Journal of Geology, v. 90, p. 393–413.
Lowenstam, H. A., and Epstein, S., 1954, Paleotemperatures of the post-Aptian Cretaceous as determined by the oxygen isotope method: Journal of Geology, v. 62, p. 207–248.
Ludwig, W. J., Krasheninnikov, V. A., et al., 1983, Initial reports of the Deep Sea Drilling Project: Washington, D.C., U.S. Government Printing Office, v. 71, 1187 p.
MacLeod, K. G., 1994, Bioturbation, inoceramid extinction, and mid-Maastrichtian ecological change: Geology, v. 22, p. 139–142.
Matter, A., Douglas, R. G., and Perch-Nielsen, K., 1975, Fossil preservation, geochemistry and diagenesis of pelagic carbonates from Shatsky Rise, northwest Pacific, *in* Larson, R. L., Moberly, R., et al., Initial reports of the Deep Sea Drilling Project: Washington, D.C., U.S. Government Printing Office, v. 32, p. 891–922.
McArthur, J. M., Thirlwall, M. F., Chen, M., Gale, A. S., and Kennedy, W. J., 1993, Strontium isotope stratigraphy in the Late Cretaceous: Numerical calibration of the Sr isotope curve, and intercontinental correlation for the Campanian: Paleoceanography, v. 8, p. 859–873.
McArthur, J. M., Kennedy, W. J., Chen, M., Thirlwall, M. F., and Gale, A. S., 1994, Strontium isotope stratigraphy for Late Cretaceous time: Direct numerical calibration of the Sr isotope curve based on the U.S. Western Interior: Palaeogeography, Palaeoclimatology, Palaeoecology, v. 108, p. 95–119.
Naydin, D. P., Teys, R. V., and Zadorozhnyy, I. K., 1966, Isotopic paleotemperatures of the Upper Cretaceous in the Russian Platform and other parts of the USSR: Geochemistry International, v. 3, p. 1038–1051.
Nelson, C. S., 1986, Lithostratigraphy of Deep Sea Drilling Project Leg 90 drill sites in the southwest Pacific: An overview, *in* Kennett, J. P., von der Borch, C. C., et al., Initial reports of the Deep Sea Drilling Project: Washington, D.C., U.S. Government Printing Office, v. 90, p. 1471–1491.
Oberhansli, H., 1986, Latest Cretaceous–early Neogene oxygen and carbon isotopic record at DSDP sites in the Indian Ocean: Marine Micropaleontology, v. 10, p. 91–115.
Olivero, E. B., Gasparini, Z., Rinaldi, C. A., and Scasso, R., 1991, First record of dinosaurs in Antarctica (Upper Cretaceous, James Ross Island): Palaeogeographic implications, *in* Thomson, M. R. A., Crame, J. A., and Thomson, J. W., eds., Geological evolution of Antarctica: London, United Kingdom, Cambridge University Press, p. 617–622.
Pisciotti, K. A., 1981, Distribution, thermal histories, isotopic compositions, and reflection of siliceous rocks recovered by the Deep Sea Drilling Project, *in* Warme, J. E., Douglas, R. G., and Winterer, E. L., eds., The Deep Sea Drilling Project: A decade of progress: Society of Economic Paleontology and Mineralogy Special Publication 32, p. 129–148.
Richter, F. M., and DePaolo, D. J., 1988, Diagenesis and Sr isotopic evolution of seawater using data from DSDP 590B and 575: Earth and Planetary Sciences Letters, v. 90, p. 382–384.
Rind, D., and Chandler, M., 1991, Increased ocean heat transport and warmer climate: Journal of Geophysical Research, v. 96, p. 7437–7461.
Saito, T., and Van Donk, J., 1974, Oxygen and carbon isotope measurements of Late Cretaceous and early Tertiary foraminifera: Micropaleontology, v. 20, p. 152–177.
Saltzman, E. S., and Barron, E. J., 1982, Deep circulation in the Late Cretaceous: Oxygen isotope paleotemperatures from *Inoceramus* remains in DSDP cores: Palaeogeography, Palaeoclimatology, Palaeoecology, v. 40, p. 167–181.
Savin, S. M., Abel, L., Barrera, E., Hodell, D. A., Keller, G., Kennett, J. P., Killingley, J. S., Murphy, M. E., and Vincent, E., 1985, The evolution of Miocene surface and near-surface marine temperatures: Oxygen isotopic evidence, *in* Kennett, J. P., ed., The Miocene ocean: Paleoceanography and biogeography: Geological Society of America Memoir 163, p. 49–82.
Schlanger, S. O., and Douglas, R. G., 1974, The pelagic ooze-chalk-limestone transition and its implications for marine stratigraphy, *in* Hsü, K. J., and Jenkyns, H. C., Pelagic sediments: On land and under the sea: International Association for Sedimentologists Special Publication 1, p. 117–148.
Schneider, S. H., Thompson, S. L., and Barron, E. J., 1985, Mid-Cretaceous continental surface temperatures: Are high CO_2 concentrations needed to simulate above-freezing winter conditions?, *in* Sundquist, E. T., and Broecker, W. S., eds., The carbon cycle and atmospheric CO_2: Natural variations Archean to present: American Geophysical Union Geophysical Monograph 32, p. 554–560.
Scholle, P. A., and Arthur, M. A., 1980, Carbon isotope fluctuations in Cretaceous pelagic limestones: Potential stratigraphic and petroleum exploration tool: American Association of Petroleum Geologists Bulletin, v. 64, p. 67–87.
Schrag, D. P., DePaolo, D. J., and Richter, F. M., 1992, Oxygen isotope exchange in a two-layer model of oceanic crust: Earth and Planetary Sciences Letters, v. 111, p. 305–317.
Sellwood, B. W., Price, G. D., and Valdes, P. J., 1994, Cooler estimates of Cretaceous temperatures: Nature, v. 370, p. 453–455.
Shackleton, N. J., and Kennett, J. P., 1975, Paleotemperature history of the Cenozoic and the initiation of Antarctic glaciation: Oxygen and carbon isotope analysis in DSDP Sites 277, 279, and 280, *in* Kennett, J. P., Houtz, R. E., et al., Initial reports of the Deep Sea Drilling Project 29: Washington, D.C., U.S. Government Printing Office, p. 743–755.
Shackleton, N. J., and Vincent, E., 1978, Oxygen and carbon isotope studies in Recent foraminifera from the southeast Indian Ocean: Marine Micropaleontology, v. 3, p. 1–13.
Sliter, W. V., 1972, Cretaceous foraminifers—Depth habitats and their origin: Nature, v. 239, p. 514–515.
Sliter, W. V., 1977, Cretaceous foraminifers from the southwestern Atlantic Ocean, Leg 36, Deep Sea Drilling Project, *in* Barker, P. F., Dalziel, I. W. D., et al., Initial reports of the Deep Sea Drilling Project: Washington, D.C., U.S. Government Printing Office, v. 36, p. 519–573.
Sliter, W. V., 1995, Cretaceous planktonic foraminifers from Sites 865, 866, and 869: A synthesis of Cretaceous pelagic sedimentation in the central Pacific Ocean basin, *in* Winterer, E. L., Sager, W. W., Firth, J. V., et al., Proceedings of the Ocean Drilling Program, scientific results 143: College Station, Texas, Ocean Drilling Program, in press.
Sohl, N. F., 1969, North American Cretaceous biotic provinces delineated by gastropods, *in* Proceedings of the North American Paleontologic Convention II: Lawrence, Kansas, Allen Press, p. 1610–1637.
Spaeth, C., Hoefs, J., and Vetter, U., 1971, Some aspects of isotopic composition of belemnites and related paleotemperatures: Geological Society of America Bulletin, v. 82, p. 3139–3150.
Spero, H. J., and Williams, D. J., 1989, Opening the carbon isotope "vital effect" black box 1. Seasonal temperatures in the euphotic zone: Paleoceanography, v. 4, p. 593–601.
Spicer, R. A., and Parrish, J. T., 1986, Paleobotanical evidence for cool north polar climates in middle Cretaceous (Albanian–Cenomanian) time: Geology, v. 14, p. 703–706.
Spicer, R. A., and Parrish, J. T., 1987, Plant megafossils, vertebrate remains and paleoclimate of the Kogosukruk Tongue (Late Cretaceous), North Slope, Alaska: U.S. Geological Survey Circular 998, p. 47–48.
Stevens, G. R., and Clayton, R. N., 1971, Oxygen isotope studies on Jurassic and Cretaceous belemnites from New Zealand and their biogeographic significance: New Zealand Journal of Geology and Geophysics, v. 14, p. 829–897.
Sugarman, P. J., Miller, K. G., Bukry, D., and Feigenson, M. D., 1995, Uppermost Campanian–Maestrichtian strontium isotopic, biostratigraphic, and sequence stratigraphic framework of the New Jersey Coastal Plain: Geological Society of America Bulletin, v. 107, p. 19–37.
Thierstein, H. R., 1974, Calcareous nannoplankton—Leg 26, Deep Sea Drilling Project, *in* Davies, T. A., Luyendyk, B. P., et al., Initial reports of the Deep Sea Drilling Project: Washington, D.C., U.S. Government Printing Office, v. 26, p. 619–667.
Thierstein, H. R., and Roth, P. H., 1991, Stable isotopic and carbonate cyclicity in Lower Cretaceous deep-sea sediments: Dominance of diagenetic effects: Marine Geology, v. 97, p. 1–34.
Vakhrameev, V. A., 1975, Main features of phytogeography of the globe in Jurassic and Early Cretaceous time: Paleontological Journal, v. 2, p. 247–255.
Varentsov, I. M., Sakharov, B. A., and Eliseeva, T. G., 1983, Clay components of post-Middle Jurassic sediments of the southwest Atlantic, Deep Sea Drilling Project, Leg 71: Depositional history and transformations, *in* Ludwig, W. J., Krasheninnikov, V. A., et al., eds., Initial reports of the Deep Sea Drilling Project: Washington, D.C., U.S. Government Printing Office, v. 71, p. 351–367.
Veevers, J. J., 1986, Break-up of Australia and Antarctica estimated at mid-Cretaceous (95 + or − 5 Ma) from magnetic and seismic data at the continental margin: Earth and Planetary Science Letters, v. 77, p. 91–99.
Veevers, J. J., 1987, Earth history of the southeast Indian Ocean and the conjugate margins of Australia and Antarctica: Royal Society of New South Wales Journal and Proceedings, v. 120, p. 57–70.
Veizer, J., 1974, Chemical diagenesis of belemnite shells and possible consequences for paleotemperature determinations: Neues Jahrbuch für Geologie und Palaontologie, Abhandlungen, v. 147, p. 91–111.
Wefer, G., and Berger, W. H., 1991, Isotope paleontology: Growth and composition of extant calcareous species: Marine Geology, v. 100, p. 207–248.
Wind, F. H., and Wise, S. W., Jr., 1983, Correlation of upper Campanian–lower Maestrichtian calcareous nannofossil assemblages in drill and lower piston cores from the Falkland Plateau, southwest Atlantic Ocean, *in* Ludwig, W. J., Krasheninnikov, V. A., et al., eds., Initial reports of the Deep Sea Drilling Project: Washington, D.C., U.S. Government Printing Office, v. 71, p. 551–563.

Wise, S. W., Jr., 1983, Mesozoic and Cenozoic nannofossils recovered by Deep Sea Drilling Project Leg 71 in the Falkland Plateau region, Southwest Atlantic Ocean, *in* Ludwig, W. J., Krashenninikov, V. A., et al., eds., Initial reports of the Deep Sea Drilling Project: Washington, D.C., U.S. Government Printing Office, v. 71, p. 481–550.

Wise, S. W., Jr., and Wind, F. H., 1977, Mesozoic and Cenozoic calcareous nannofossils recovered by DSDP Leg 36 drilling on the Falkland Plateau, southwest Atlantic sector of the southern ocean, *in* Barker, P. F., Dalziel, I. W. D., et al., Initial reports of the Deep Sea Drilling Project: Washington, D.C., U.S. Government Printing Office, v. 36, p. 269–491.

Wolfe, J. A., and Upchurch, G. R. , Jr., 1987, North American nonmarine climates and vegetation during the Late Cretaceous: Palaeogeography, Palaeoclimatology, Palaeoecology, v. 61, p. 33–77.

Woo, K. S., Anderson, T. F., Railsback, L. B., and Sandberg, P. A., 1992, Oxygen isotope evidence for high-salinity surface seawater in the mid-Cretaceous Gulf of Mexico: Implications for warm, saline deepwater formation: Paleoceanography, v. 7, p. 673–685.

Zachos, J. C., Stott, L. D., and Lohmann, K. C., 1994, Evolution of early Cenozoic marine temperatures: Paleoceanography, v. 9, p. 353–387.

MANUSCRIPT RECEIVED BY THE SOCIETY JULY 21, 1994
REVISED MANUSCRIPT RECEIVED FEBRUARY 28, 1995
MANUSCRIPT ACCEPTED MARCH 11, 1995

Printed in U.S.A.

Nd isotopic constraints on sediment sources of the Ouachita-Marathon fold belt

James D. Gleason*
P. Jonathan Patchett
William R. Dickinson
Joaquin Ruiz

Department of Geosciences, University of Arizona, Tucson, Arizona 85721

ABSTRACT

Nd isotopes for the overthrust deep-marine Ouachita-Marathon sedimentary assemblage of Arkansas-Oklahoma and west Texas, and associated Paleozoic shelf and foreland deposits, resolve into three distinct populations: (1) Lower to Middle Ordovician, $\varepsilon_{Nd} = -13$ to -16 (average $T_{DM} = 2.0$ Ga); (2) Upper Ordovician to Pennsylvanian, $\varepsilon_{Nd} = -6$ to -10 (average $T_{DM} = 1.6$ Ga); and (3) Mississippian tuffs, $\varepsilon_{Nd} = -1$ to -3 (average $T_{DM} = 1.1$ Ga). A rapid shift in ε_{Nd} from -15 (passive margin shales) to -7 (orogenic turbidites) in the Ouachita assemblage at ca. 450 Ma implies termination of craton-dominated sources and the emergence of the Appalachian orogen as the primary source of sediment for sea floor lying south of North America. This connection is reinforced by Nd isotopes in Ordovician-Silurian turbidites from both the Ouachita assemblage and the southern Appalachian Sevier-Martinsburg (Taconic) foredeep, which are identical ($\varepsilon_{Nd} = -7$ to -9). The post–450 Ma Ouachita assemblage falls along a single Nd isotopic trend that, significantly, is not deflected by onset of Carboniferous flysch ($\varepsilon_{Nd} = -7$ to -10) sedimentation nor by associated regional volcanism. The less negative ε_{Nd} (−2) of Mississippian ash-flow tuffs that erupted from arc(s) to the south probably resulted from isotopic mixing of old (Precambrian) crust with young, mantle-derived components within a continental margin arc. There is little isotopic, trace element, or petrographic evidence for any significant volcaniclastic detritus in the Carboniferous turbidites, indicating that volcanic arc sources were minimal.

Nd isotopes in fluvio-deltaic strata of the Ouachita-Appalachian foreland and continental interior, that is, Arkoma, Illinois, and Black Warrior basins ($\varepsilon_{Nd} = -7$ to -10), imply that continental margin pathways and interior basins received the same detritus as the Ouachita trough by Pennsylvanian time. These data are consistent with a composite Carboniferous Ouachita submarine fan complex built down the axis of a remnant ocean basin from varied mature/immature delivery systems tapping dominantly Appalachian fold-thrust belt sources to the east (Graham et al., 1975). Carboniferous turbidites from the Marathon fold belt (west Texas), which are isotopically similar ($\varepsilon_{Nd} = -8$ to -11) to Ouachita turbidites, may have been ultimately derived from similar sources; however, they probably do not represent merely distal turbidites of a Ouachita fan complex. It is suggested that dominantly Appalachian-derived detritus, augmented by uplifted plutonic and fold-thrust belt sources south of the Marathon basin, was swept up into subduction complexes on the north side of the approaching arc and recycled along the collision zone.

INTRODUCTION

Plate tectonic models for the late Paleozoic Ouachita (Hercynian) orogenic belt at the southern margin of North America generally place it in the context of a complete Wilson cycle (Viele and Thomas, 1989), but because most of it lies buried in the subsurface, many important tectonic relations are obscured. Recognition of the Ouachita orogenic belt in Mexico is important for delineating the limits of the Cordilleran miogeocline, the southern extension of the North American craton, and the subsequent tectonic assembly of Mexico (e.g., Stewart, 1988; Shurbet and Cebull, 1987; Handschy et al., 1987; Campa and Coney, 1983), but it has been hampered by extensive Cenozoic volcanic cover and, where exposed, by Mesozoic-Cenozoic metamorphism and deformation. Tectonic linkages with the Appalachian orogen and the Caribbean region are also obscured by Jurassic Gulf of Mexico rifting and subsequent burial of the continental margin (e.g., Thomas, 1989; Dickinson and Coney, 1980). The landmass(es) that collided with North America to produce the Ouachita orogenic belt may have included several tectonic elements presently distributed throughout the Gulf of Mexico–Caribbean region (e.g., Pindell, 1985; Campa and Coney, 1983; Yañez et al., 1991), but such speculations remain essentially without constraints; likewise, the landmass that separated from the late Proterozoic/early Paleozoic Ouachita rifted margin is also unknown, though much importance has been affixed to its identity in the context of global tectonic reconstructions (e.g., Dalziel et al., 1994; Hoffman, 1991). Evidence suggests, however, that a long-lived proto-Atlantic ocean basin (Iapetus) resided south of North America through most of Paleozoic time (Scotese, 1984).

Despite these difficulties, a nearly complete Paleozoic stratigraphic record is preserved in the overthrust deep-marine Ouachita sedimentary assemblage, which documents the transition from a

*Present address: Lunar and Planetary Laboratory, University of Arizona, Tucson, Arizona 85721.

Data Repository item 9538 contains additional material related to this article.

GSA Bulletin; October 1995; v. 107; no. 10; p. 1192–1210; 9 figures; 4 tables.